



**STRUCTURAL SYSTEMS
RESEARCH PROJECT**

Report No.
SSRP0903

**STRUCTURAL RESPONSE OF NEAR
SURFACE MOUNTED CFRP
STRENGTHENED REINFORCED
CONCRETE BRIDGE DECK
OVERHANG**

by

ANNA B. PRIDMORE

VISTASP M. KARBHARI

Final Report Submitted to the California Department of
Transportation Under Contract No. 59A0630.

November 2008

Department of Structural Engineering
University of California, San Diego
La Jolla, California 92093-0085
&
University of Alabama in Huntsville
Huntsville, AL 35899

University of California, San Diego
Department of Structural Engineering
Structural Systems Research Project

Report No. SSRP0903

**Structural Response of Near Surface Mounted CFRP
Strengthened Reinforced Concrete Bridge Deck Overhang**

by

Anna B. Pridmore
Graduate Student Researcher

Vistasp M. Karbhari
Professor of Structural Engineering

Final Report submitted to the California Department of Transportation
Under Contract No. 59A0630.

Department of Structural Engineering
University of California, San Diego
La Jolla, California 92093-0085

&

University of Alabama in Huntsville
Huntsville, AL 35899

November 2008

1. Report No.		2. Government Accession No.		3. Recipient's Catalog No.	
4. Title and Subtitle Structural Response of Near Surface Mounted CFRP Strengthened Reinforced Concrete Bridge Deck Overlay				5. Report Date November 2008	
				6. Performing Organization Code	
7. Author(s) Anna Pridmore and Vistasp M. Karbhari				8. Performing Organization Report No. UCSD / SSRP- 0903	
9. Performing Organization Name and Address University of California, San Diego La Jolla, California 92093-0085 & University of Alabama in Huntsville Huntsville, Al 35899				10. Work Unit No. (TRAIS)	
				11. Contract or Grant No. 59A0630	
12. Sponsoring Agency Name and Address California Department of Transportation Engineering Service Center 1801 30 th St., West Building MS-9 Sacramento, California 95807				13. Type of Report and Period Covered Final Report	
				14. Sponsoring Agency Code	
15. Supplementary Notes Prepared in cooperation with the State of California Department of Transportation.					
16. Abstract This report presents the results from an experimental investigation which explores the change in structural response due to the addition of near-surface-mounted (NSM) carbon fiber reinforced polymer (CFRP) reinforcement for increasing the capacity of the edge region of a reinforced concrete bridge deck. The motivation for rehabilitating bridge deck overhangs using NSM reinforcement is to increase the load carrying capacity of the region so that the overhang can accommodate the larger than designed for loads caused by the installation of sound barrier walls onto the edges of the bridge deck. The experimental testing of an as-built reinforced concrete specimen without FRP was used as the baseline test to evaluate the effectiveness of the NSM CFRP strengthening scheme. Details regarding the capacity calculations, experimental setup, testing protocol and experimental results for the as-built specimen and FRP rehabilitated specimen are discussed in this report. This report also presents the NSM CFRP strengthening design options examined for achieving the desired capacity increase and evaluates the change in structural response of the rehabilitated system as compared to the as-built test specimen.					
17. Key Words Composite, Strengthening, Near Surface mounted, Reinforcement, Overhang, Sound Walls				18. Distribution Statement No restrictions	
19. Security Classification (of this report) Unclassified		20. Security Classification (of this page) Unclassified		21. No. of Pages 174	22. Price

DISCLAIMER

The contents of this report reflect the views of the authors who are responsible for the facts and accuracy of the data presented herein. The contents do not necessarily reflect the official views or policies of the State of California or the Federal Highway Administration. This report does not constitute a standard, specification or regulation.

TABLE OF CONTENTS

Abstract		iv
1	Introduction	1
1.1	Project-Specific Need for FRP Rehabilitation	1
1.2	Methods of FRP Rehabilitation	2
1.3	Near Surface Mounted FRP Reinforcement	3
1.3.1	Variations	4
1.3.2	Prior Use	5
1.3.3	Available Codes and Specifications	6
2	Goals and Objectives	7
3	Overall Experimental Setup	8
3.1	Specimen Geometry and Construction	8
3.2	Loading Setup	10
4	As-Built Test	12
4.1	Demand Calculations	12
4.2	Capacity Calculations	13
4.3	Instrumentation	15
4.4	Loading Protocol	16
4.5	Experimental Results	18
4.6	Comparison with Theory	26
5	Rehabilitated Test	27
5.1	Calculations for Potential CFRP NSM Strengthening Schemes	27
5.2	Options for Rehabilitation	29
5.3	Rehabilitation Construction	35
5.4	Capacity Calculations	38
5.5	Instrumentation	39
5.6	Loading Protocol	42
5.7	Experimental Results	43
5.8	Comparison with Theory	54
5.9	Comparison with As-Built	55
6	Summary of Results and Recommendations for Future Research	60
7	References	62

ABSTRACT

This report presents the results from an experimental investigation which explores the change in structural response due to the addition of near-surface-mounted (NSM) carbon fiber reinforced polymer (CFRP) reinforcement for increasing the capacity of the edge region of a reinforced concrete bridge deck. The motivation for rehabilitating bridge deck overhangs using NSM reinforcement is to increase the load carrying capacity of the region so that the overhang can accommodate larger than designed for loads caused by the installation of sound barrier walls onto the edges of the bridge deck. The experimental testing of an as-built reinforced concrete specimen without FRP was used as the baseline test to evaluate the effectiveness of the NSM CFRP strengthening scheme. Details regarding the capacity calculations, experimental setup, testing protocol and experimental results for the as-built specimen and FRP rehabilitated specimen are discussed in this report. This report also presents the NSM CFRP strengthening design options examined for achieving the desired capacity increase and evaluates the change in structural response of the rehabilitated system as compared to the as-built test specimen.

1. Introduction

1.1 Project-Specific Need for FRP Rehabilitation

In order to improve the quality of life for residents who live close to major highways, Caltrans is installing sound barriers along many roadways in California. When these sound barrier walls are installed onto bridges, they are placed on the edge of the deck slab overhang, on top of traffic barriers. The sound barrier walls are often made of concrete or masonry, which add additional loads to the edges of the bridges in excess of the original design loads. The current solution employed is to remove the entire edge region of the bridge deck and rebuild it with additional reinforcement to accommodate the increased loading. However, this process necessitates road closures and is time consuming and costly. An alternative to replacement of the bridge deck slab overhang is strengthening of the overhang through the use of fiber reinforced polymers (FRPs). FRPs have been shown to be very beneficial for a variety of civil applications including strengthening of bridge decks because of their high strength to weight ratio, tailor able properties and potential for enhanced durability and corrosion resistance over traditional structural materials. The ease of installation of FRP rehabilitation systems as compared to traditional strengthening materials and methods allows for reduced highway closure time and disruption of traffic flow.

The current research is a preliminary experimental investigation to explore the application of composites for increasing the capacity of the overhang region of the bridge deck to accommodate the larger loads caused by the addition of the sound barrier walls. Under the scope of the project the aim was to test a single method of rehabilitation in order to provide preliminary validation of the technique. The overall project is divided into two phases with this being the first phase. The second phase includes a detailed literature review and state-of-the-art report in addition to a focused building-block based approach to the assessment of the use of near surface mounted reinforcement aimed at the development of a design guideline for Caltrans. It is emphasized that the current research was based on the use of an existing specimen and hence the test does not directly mimic some cases that may be under consideration. The goal, as mentioned earlier, was to show viability, rather than to provide a direct set of design guidelines. However, the research

was based on submission of detailed test plans and alternatives to Caltrans along with recommendations for the rehabilitation. Caltrans approval was obtained prior to initiation of the test program and was again obtained for the down-selected rehabilitation option.

1.2 Methods of FRP Rehabilitation

FRP rehabilitation can serve to efficiently strengthen, repair or seismically retrofit a wide variety of existing civil structures. The use of FRP reinforcement which is bonded to the tension side of concrete beams, slabs, or girders can provide improved flexural strength whereas use of the FRP reinforcement bonded to the sides of girders and beams can provide additional shear strength for the structure. FRP reinforcement may also be used to wrap columns in order to provide confinement for the concrete and additional ductility for the column during a seismic event. Figure 1 shows a variety of rehabilitation methods applied to columns which involve the use of FRP reinforcement.

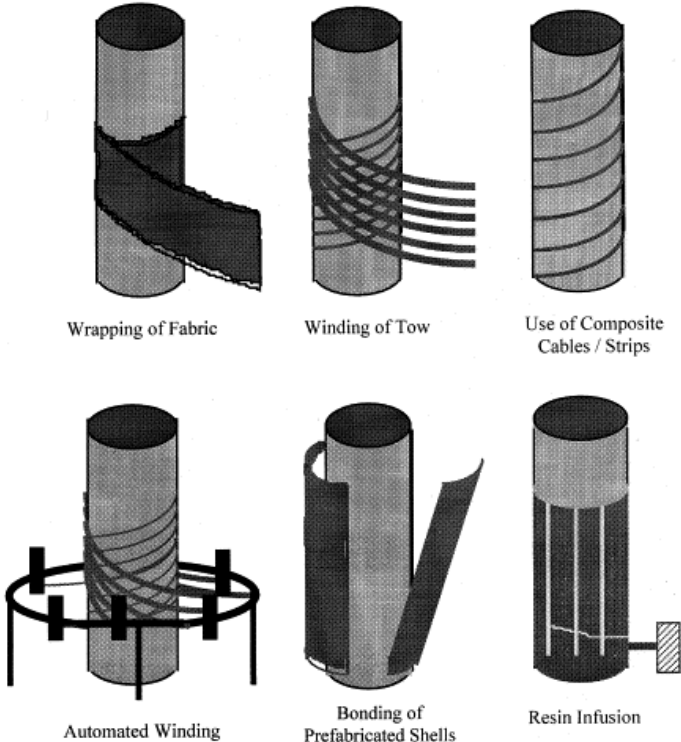


Figure1: Methods of FRP rehabilitation for columns [1]

The two main categories for FRP rehabilitation techniques are externally bonded FRP systems and near-surface-mounted FRP systems. Externally bonded FRP systems include but are not limited to wet layup processes, bonding of pre-cured FRP profiles to a structure, resin infusion of dry fabric after installation of the FRP, and use of prepreg sheets [2]. An application of externally bonded prefabricated strips and externally bonded on site impregnated fabric laminates for the rehabilitation of bridge deck slabs are shown in Figures 2(a) and (b) respectively.



a) Pultruded strips



b) Wet layup fabric laminates

Figure 2: Rehabilitation of bridge deck slabs using externally bonded FRP reinforcement [3]

1.3 Near Surface Mounted FRP Reinforcement

Near surface mounted FRP systems are a recent development, although the general use of the strategy can be traced to the use of steel rebar in surface cut grooves in Europe in the 1950s. This approach involves the installation of the FRP reinforcement into pre-cut grooves in the cover region of the concrete substrate to be strengthened. The reinforcement is thus placed inside the concrete substrate and covered with other material (cementitious or a polymer adhesive) rather than being adhesively bonded to the surface. The use of near-surface-mounted (NSM) FRP reinforcement for rehabilitation has a number of advantages over the more common externally bonded FRP reinforcement. These advantages include the potential for reduced site installation work, since surface preparation beyond the creation of grooves for the FRP is no longer required, the reduced likelihood of debonding failures from the concrete surface due to significantly improved anchoring ability and improved protection from mechanical damage provided by

recess of the NSM reinforcement into the concrete surface [4,5]. The use of near surface mounted FRP rehabilitation techniques provide particular advantages for flexural strengthening of the negative moment region of reinforced concrete slabs and decks. In these applications, the top surface of the deck may be subject to harsh environmental and use conditions, which would require the FRP reinforcement to be surrounded by a protective cover. This would more difficult to achieve using externally bonded strips whereas the near surface mounted reinforcement is already embedded and therefore not exposed to these influences.

1.3.1 Variations

FRP reinforcement used for near-surface-mounted applications can be manufactured in a wide variety of shapes including round, oval, square and rectangular bars, as well as strips with varying width-to-thickness ratios. Figure 3 shows a variety of different FRP bars and strips that are commonly available for NSM applications.



Figure 3: A selection of types of FRP bars and strips available for NSM applications [4]

Carbon fiber reinforced polymer composite NSM reinforcement is the primary type of FRP material used to rehabilitate concrete structures because of the higher tensile strength and tensile modulus of carbon over glass or aramid, as well as the inertness of the fiber which reduces the effect of concrete based alkalinity on the FRP itself. These superior tensile properties allow for a smaller cross-sectional area CFRP bar to be used over a GFRP or AFRP bar with the same tensile capacity, which has additional constructability benefits by reducing the risk of interfering with the internal steel reinforcement.

It should be noted that while the initial use of NSM was with circular bars the transition to rectangular strips was predicated on the desire to attain higher strains in the reinforcing prior to debonding. It has been proven that all other factors being equal, NSM strips have higher average bond strengths than circular bars because of the development of a three-dimensional distribution of bond stresses in the surrounding concrete. Further, in the case of round bars, forces due to radial stresses can induce tensile forces that can force the bar out of the groove resulting in splitting and bond failure. It should also be noted that since strips have significantly larger ratios of perimeter to cross-sectional area than circular or rectangular rods bond stresses are lower. The primary failure modes for NSM include concrete crushing, FRP rupture, adhesive splitting, concrete splitting, combined splitting, and separation of the concrete cover region. These are exacerbated by round and rectangular rods as compared to flat strips due to the greater depth of embedment and larger cross-sectional area as compared to surface area. It should also be emphasized that while the technique is extremely simple the use of square bars and rods requires use of larger and deeper grooves than flat strips placed horizontally in order to achieve the same efficiency. A significantly more in-depth review of differences and modes of failure will be reported in the Phase-2 report.

1.3.2 Prior Use

While NSM FRP has been used successfully for flexural strengthening of concrete beams [6,7,8], there is still limited work on the use of NSM FRP applications to increase the flexural capacity of concrete slabs. Parretti and Nanni discuss a design example of flexural strengthening a one way RC slab in the negative moment region using NSM CRFP strips [9] and Bonaldo et al have researched the structural performance of a reinforced concrete slab flexurally strengthened with FRP and a steel fiber reinforced concrete overlay [10] however, despite increasing field use, there is very little detailed literature relating to experimental work on the strengthening of the negative moment region of a reinforced concrete slab.

1.3.3 Available Codes and Specifications

The Concrete Society Technical Report No. 55 discusses a variety of applications for strengthening with NSM reinforcement (TR 55, Section 6.4) and recommends that for aspects other than FRP curtailment, design of flexural strengthening with NSM reinforcement should be done using the design methods described for surface mounted reinforcement, with the allowance made to adjust the location of the reinforcement from the surface of the section to within the section such that the strains in the FRP are lowered appropriately [11]. Approaches for anchorage design are detailed and design suggestions for reducing the likelihood of different common modes of failure for NSMR are described.

ACI 440.02 makes no specific mention of strengthening using NSMR, however contains extensive information pertaining to surface mounted reinforcement. Sections pertaining to near surface mounted reinforcement are being added to the most recent edition of the ACI 440 code, however these sections are still in draft form and are not currently available [12].

The Canadian Highway Bridge Design Code includes strengthening with NSMR as part of its discussion on flexural and axial rehabilitation (Section 16.11.2) and gives resistance factors pultruded carbon, glass and aramid FRP NSMR (Section 16.5.3) [13]. This code determines NSMR anchorage lengths for flexure using the same calculation provided for internal FRP bars (Sections 16.11.2.4.4 and 16.8.4.1) and provides only a general description of failure modes for FRP strengthened systems, without mention of NSMR specific modes of failure.

2. GOALS AND OBJECTIVES

The goals of the experimental investigations presented in this report are to examine the changes in vertical load carrying capacity and structural response of a steel reinforced concrete box girder bridge deck overhang which has been rehabilitated with NSM reinforcement. The desired increase in capacity which will allow the overhang to safely accommodate the increased dead load from the addition of the soundwalls and the feasible design options for achieving this increased capacity objective must first be determined. Once the chosen CFRP NSM reinforcement strengthening scheme has been implemented and tested, the objectives of this project are to compare the rehabilitated specimen's experimental results to theoretical predictions and to the experimental results from the testing of the as-built reinforced concrete specimen without FRP.

3. OVERALL EXPERIMENTAL SETUP

3.1 Specimen Geometry and Construction

The overall test configuration used for this experimental work consists of a reinforced concrete two-cell box girder, with a center-to-center span of 1830 mm (6 ft) between each of the girders and a length of 3660 mm (12 ft) as shown in Figure 4. The specimen deck is 178 mm (7 in) thick and the distance from the stem wall to the edge of the overhang is 483 mm (19 in).

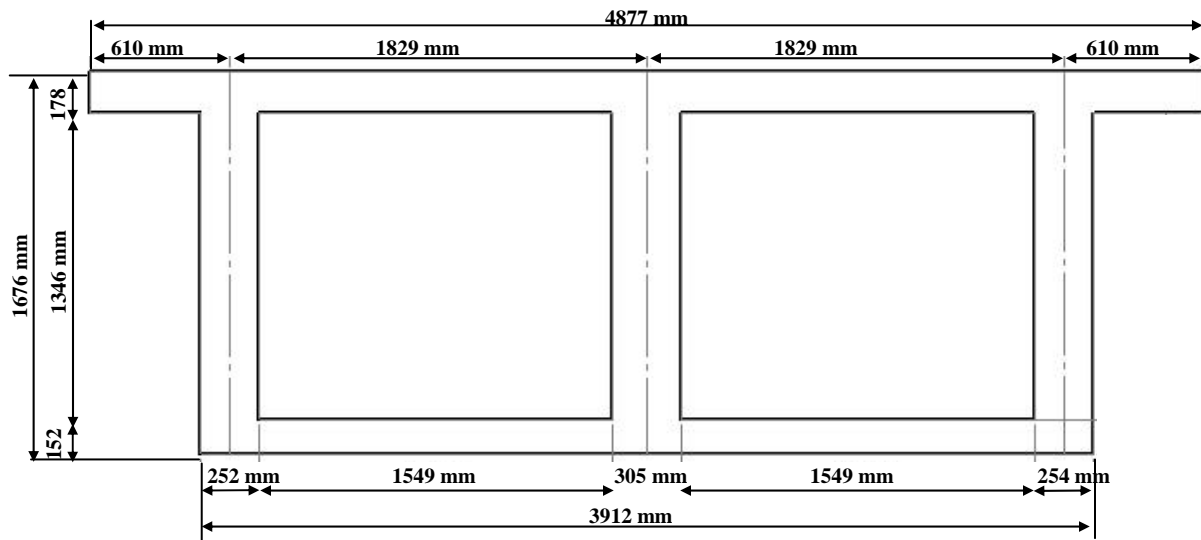


Figure 4: Overall dimensions of test specimen

All steel reinforcement used within the test specimen was designed in accordance with the AASHTO-LRFD specifications [14] and the construction practices employed mimicked field techniques. The steel reinforcement in the deck slab consisted of a top and bottom layer of #16 (#5) rebar as shown in Figure 5 with the transverse rebar spaced at 203 mm (8 in) on center and variable spacing for the longitudinal rebar in order to accommodate the location of the girder stems. The rebar used had an experimentally determined yield strength of 430 MPa (62 ksi) and an ultimate strength of 703 MPa (102 ksi). A clear cover of 25 mm (1 in) was used throughout the specimen. The specimen deck slab and the upper portion of the stems were cast in place monolithically using concrete with an average aggregate size of 127 mm (0.5 in). The concrete strength at 28 days was 34 MPa (5.0 ksi).

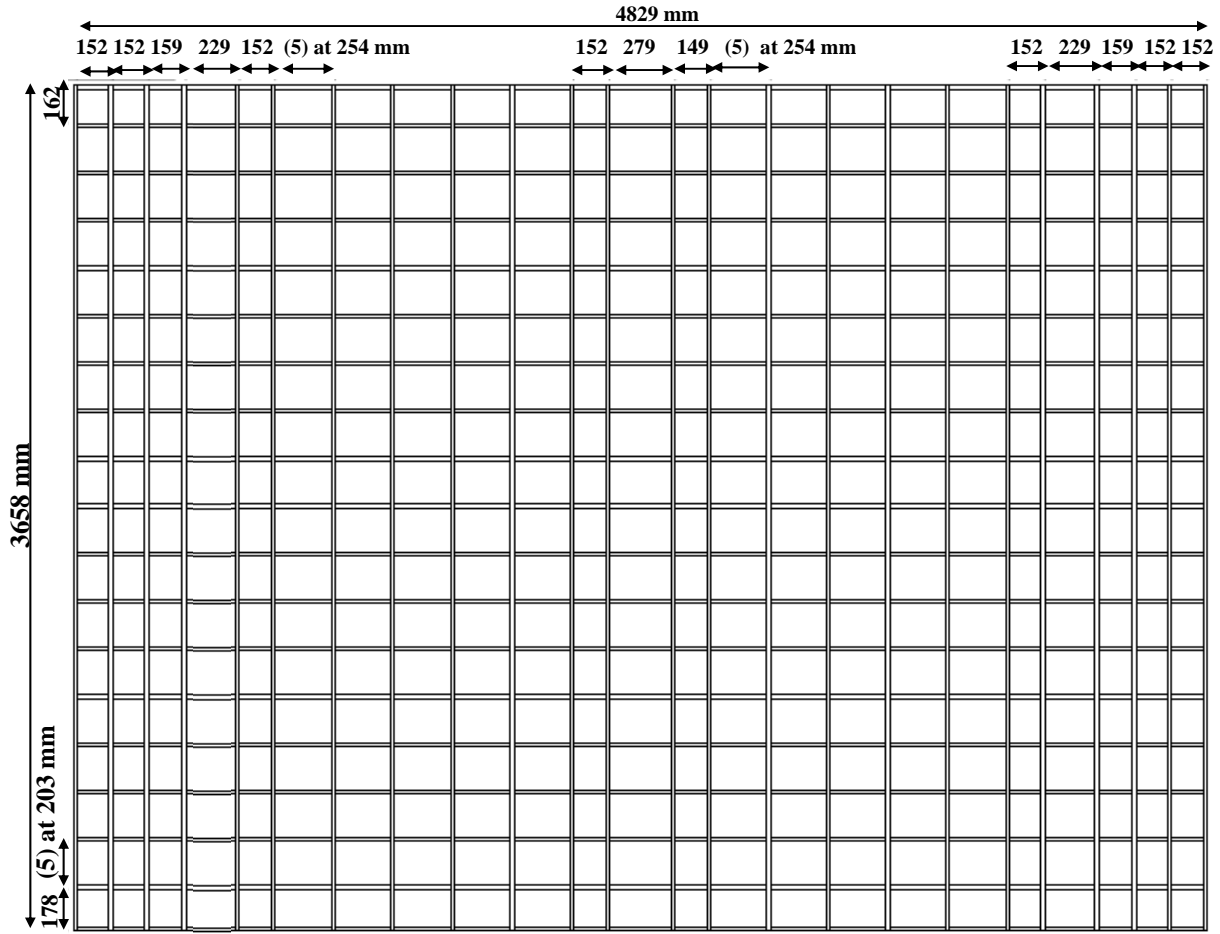


Figure 5: Reinforcement layout for deck slab

Following construction of the described test specimen, the specimen was used for a separate test series [15] after completion of which two 203 mm (8 in) deep cuts located 305 mm (12 in) apart from each other were created that ran longitudinally along the entire width of the specimen (Figure 6)). It should be noted that previous testing was restricted to loading applied at the central section of each cell and did not involve any load application or distress to the overhang regions. The two edge segments of the deck bounded by the longitudinal cuts were also removed as shown in Figure 6. The purpose of the cuts was to allow for multiple independent tests on sections of edge slab 1.68 m (5ft 6in) long.

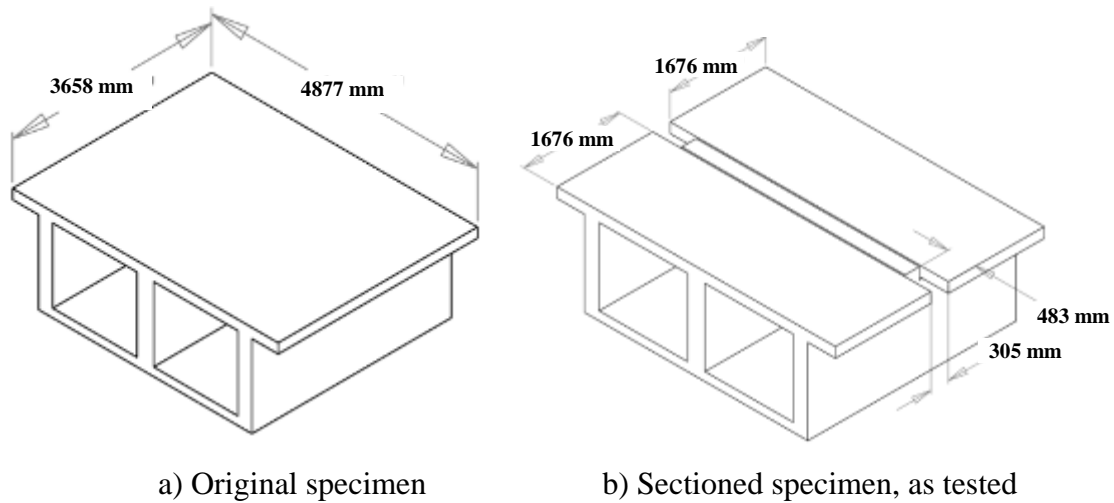


Figure 6: Test Section

3.2 Loading Setup

Vertical loads were applied to the edge region of the deck slab using two hydraulic jacks spaced 1.83 m (6 feet) apart and mounted below the strong floor of the testing facility. The load was transferred through two 44.5 mm (1 ¾ in) diameter threaded rods to a steel loading beam positioned 76 mm (3 in) on-center back from the end of the overhang section of the deck. A 51 mm (2 in) thick and 152 mm (6 in) wide elastomeric bearing pad was placed between the steel beam and the deck slab in order to reduce stress concentrations and provide more even loading of the test specimen (Figure 7). The overall test setup is shown in Figure 8.

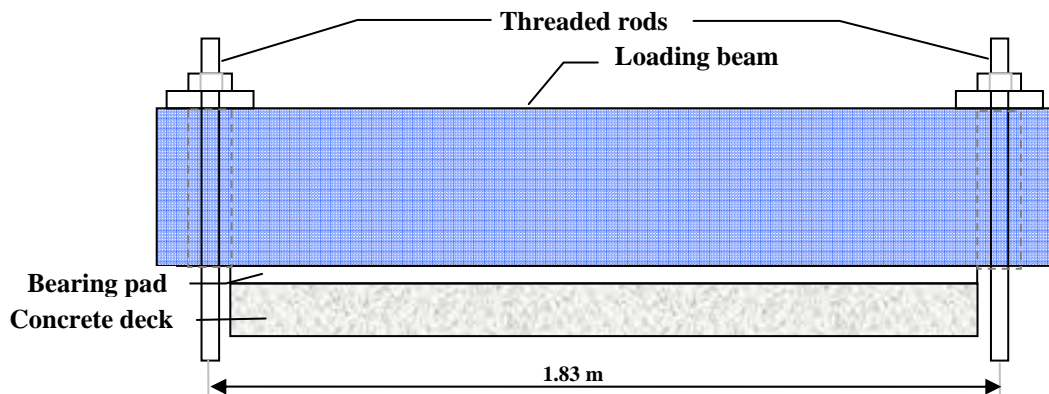


Figure 7: Test Setup Schematic

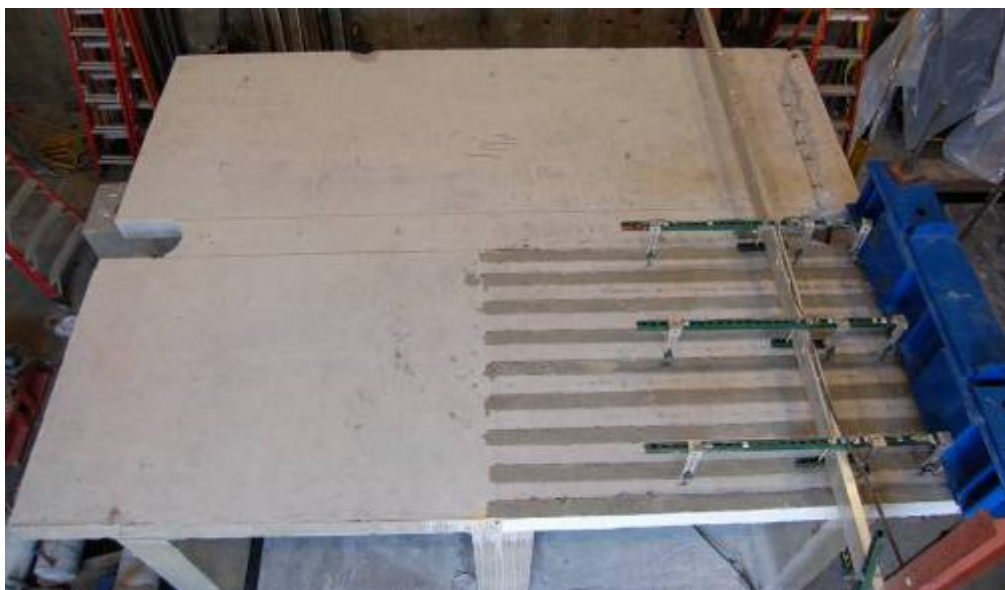


Figure 8: Overall Test Setup

4. AS-BUILT TEST

In order to establish a baseline for the effectiveness of the FRP repair, the test specimen used was isolated into separate sections as described in Section 3.1 and a portion of the concrete box girder specimen was tested as-built, without FRP rehabilitation. The following section of the report discusses the calculations, experimental setup, loading, test observations and results from the testing of this section of as-built reinforced concrete bridge deck.

4.1 Demand Calculations

The combined dead weight of a typical sound wall and traffic barrier used for bridges in California was calculated from the Caltrans' concrete masonry soundwall design on bridges as shown in Figure 9 [16]. Using this design with normal weight grout and concrete, the gravity load per unit length for the soundwall and traffic barrier were determined to be 13.5 kN/m (0.92 kip/ft) and 8.1 kN/m (0.56 kip/ft) respectively, for a combined weight per unit length of 21.6 kN/m (1.5 kip/ft). The tested section of overhang was 1600 mm (5 ft 6 in) long therefore the total load applied to the specimen from the soundwall and traffic barrier is 36.2 kN (8.25 kip).

As mentioned previously, the load was applied to the structure by two hydraulic jacks such that each jack applied half the total loading to the overhang. In equation form, this can be expressed as

$$weight_{wall_per_jack} = \frac{weight_{wall}}{2} \quad (2)$$

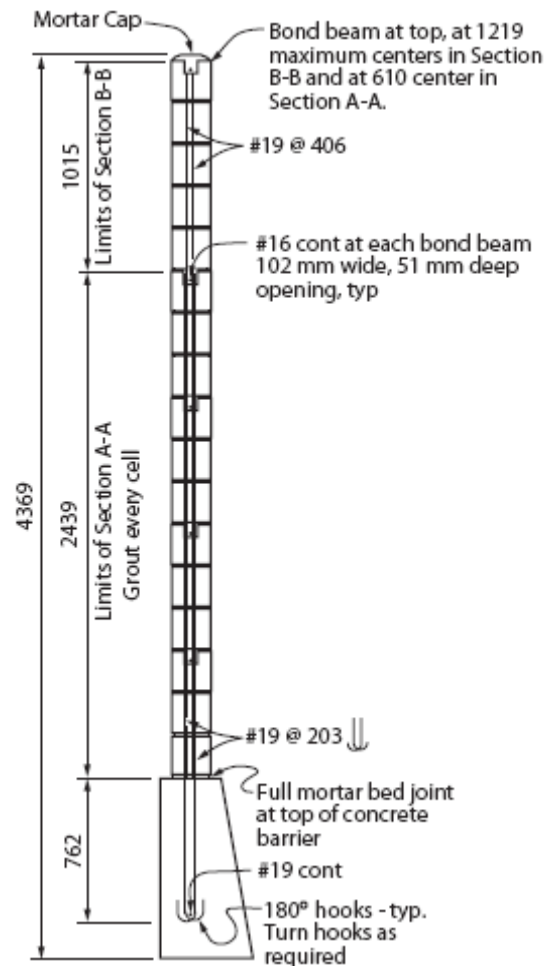


Figure 9: Standard Caltrans masonry soundwall design [16]

where $weight_{wall}$ is the total load applied to the overhang due to the combined weight of the soundwall and the traffic barrier. This yields a load per hydraulic jack of approximately 18 kN (4 kip) to represent the equivalent sound wall load, which corresponds to a distributed load of 10.7 kN/m (0.74 kip/ft).

4.2 Capacity Calculations

The shear capacity of the slab was computed according to ACI 318-08 Section 11.3 using both the general and the more detailed calculations [17]. Note that the California Bridge Design Specifications for reinforced concrete structures used by Caltrans were patterned after and are in conformity with ACI Standard 318 [18]. The general calculation for shear capacity of the slab was given by the ACI 318-08 equation 11-3 as

$$V_c = 2\sqrt{f'_c}b_wd \quad (3)$$

where f'_c is the concrete compressive strength in ksi, b_w is the width of the concrete slab in inches, and d is the distance from the extreme compression fiber to the centroid of the tensile reinforcement in inches. This equation yields a total shear capacity of 236 kN (53 kip) for the slab, which translates to an applied force of 118 kN (26.5 kip) per hydraulic jack.

The more detailed shear capacity equation is given by ACI 318-08 equation 11-5 as

$$V_c = \left(1.9\sqrt{f'_c} + 2500\rho_w \frac{V_u d}{M_u} \right) b_w d \quad (4)$$

where f'_c is the concrete compressive strength in ksi, ρ_w is the reinforcement ratio of the slab in the direction perpendicular to traffic flow, V_u and M_u are the factored moment and shear in the slab at the edge of the stem respectively, b_w is the width of the concrete slab in inches, and d is the distance from the extreme compression fiber to the centroid of the tensile reinforcement in inches. This equation yields a slightly more conservative total shear capacity of 233 kN (52.4 kip) for the slab, which translates to an applied force of 116 kN (26.2 kip) per hydraulic jack.

The moment capacity of the slab was calculated as

$$M_n = A_s f_y \left(d - \frac{a}{2} \right) \quad (5)$$

where A_s is the area of steel reinforcement in the direction perpendicular to traffic flow, f_y is the yield strength of the slab steel, d is the distance from the compression fiber to the centroid of the tensile reinforcement and a is the depth of the equivalent rectangular compression stress block. This equation yields a total moment capacity of 97.0 kN-m (71.6 kip-ft).

The equivalent force applied through the loading beam can be obtained by dividing the moment by the distance between the applied load and the edge of the stem, also known as the moment arm. The equivalent applied force per hydraulic jack was 101 kN (23 kip). Since this capacity value is lower than the computed shear capacity, it is predicted that flexural damage will govern the performance of the slab.

The moment capacity of the specimen was also found from the moment-curvature response obtained by computer program (RESPONSE 2000) to be 117.2 kN-m (85.6 kip-ft). This corresponds to a maximum load per hydraulic jack of 122 kN (27.5 kip) [19]. The moment curvature response of the as-built reinforced concrete deck slab is shown below.

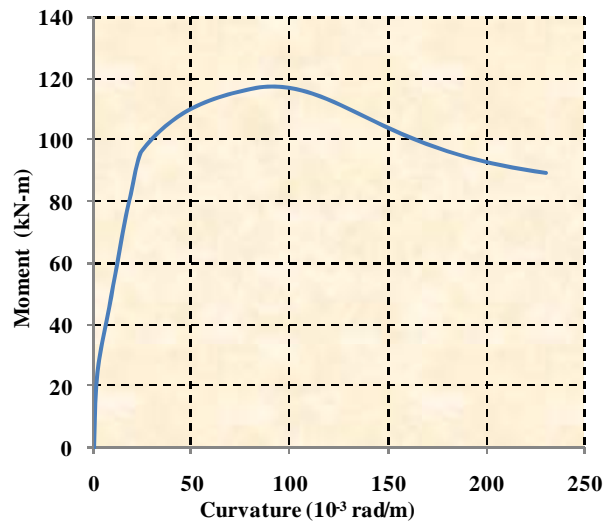


Figure 10: Moment-curvature response for as-built specimen [19]

4.3 Instrumentation

The total instrumentation for this experiment consisted of 16 linear potentiometers and 2 load cells. One central row and two outer rows, each with four linear potentiometers were used to measure the vertical deflection of the deck slab. The four linear potentiometers within each row were positioned at the midspan of the adjacent cell, above the adjacent stem, in between the stem and the loading beam, and directly below the loading beam, as shown in Figures 11(a) and (b).

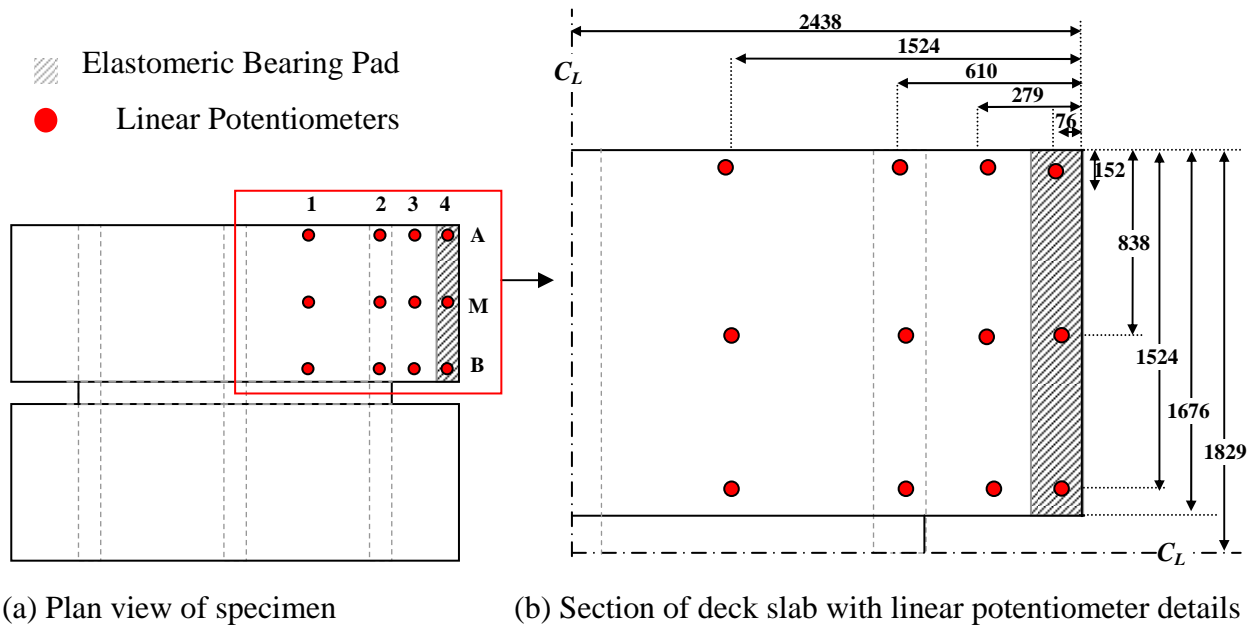


Figure 11: Position of linear potentiometers for measuring deflections of deck slab (Note: not to scale)

The deflection of the elastomeric bearing pad was measured using four linear potentiometers, with one linear potentiometer at each corner of the loading beam as shown in Figure 12.

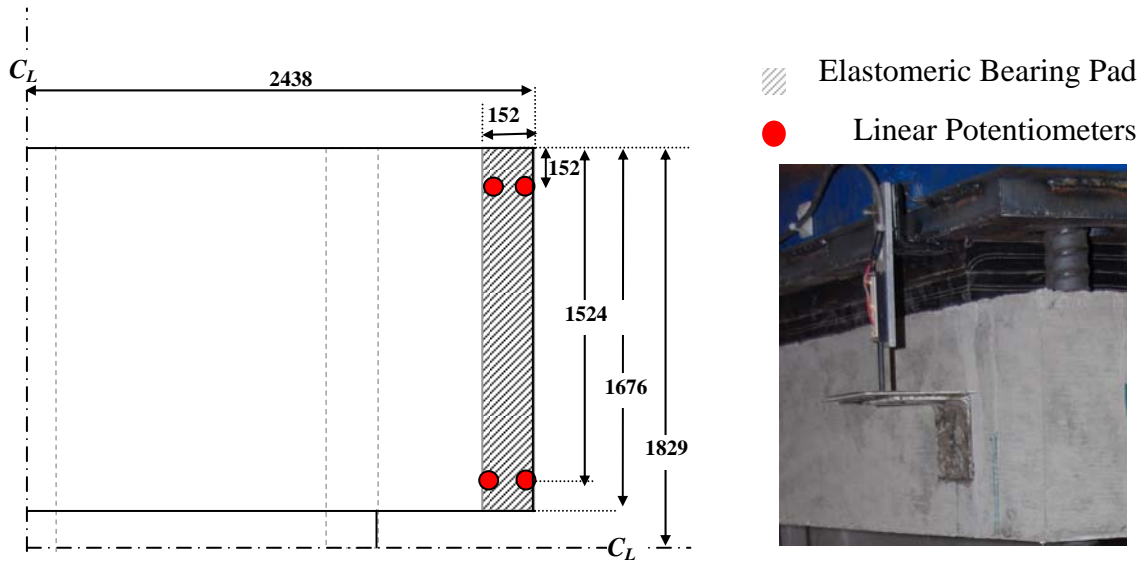


Figure 12: Position of linear potentiometers for measuring compression of bearing pad

4.4 Loading Protocol

In addition to the test setup described in Section 3.1, a 64 mm (2½ in) diameter hole was drilled through the deck of the specimen at a distance 76 mm (3 in) by 76 mm (3 in) on center away from the corner of the deck as shown in Figure 13 in order to accommodate the spacing constraints imposed by the testing setup.

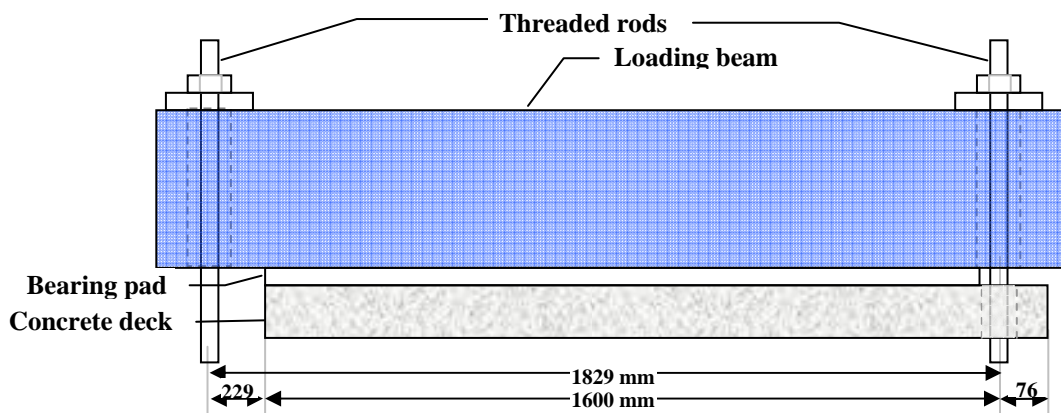


Figure 13: Specific test setup schematic for as-built specimen

The overhang of the deck slab was tested by incrementally increasing the hydraulic pressure supplied to the two hydraulic jacks, which loaded the overhang through the test setup shown in

Figure 13. Adequate time was taken between loading levels to ensure that the hydraulic pressure had stabilized and the pressure had equalized as much as possible between the two jacks. The load applied to the deck slab was monotonically increased following the loading sequence shown in Table 1. The load was held briefly at each load level so that observations could be made at each stage.

Loading step	Load per hydraulic jack		Equivalent uniform distributed load		Load level	Notes
	(kN)	(kip)	(kN/m)	(kip/ft)		
1	24	5	30.0	2.1	---	Initial load
2	36	8	45.0	3.1	2x wall load	---
3	48	11	60.0	4.1	---	---
4	60	13	75.0	5.1	---	---
5	72	16	90.0	6.2	4x wall load	---
6	84	19	105.0	7.2	---	1st set of cracks observed
7	90	20	112.5	7.7	5x wall load	---
8	96	22	120.0	8.2	---	---
9	102	23	126.3	8.7	Calculated moment capacity	2nd set of cracks observed
10	114	26	142.5	9.8	6.33x wall load	Ultimate Capacity
---	116	26	145.0	9.9	Calculated shear capacity	---

Table 1: Loading protocol for as-built test specimen

4.5 Experimental Results

The ultimate capacity of the slab was reached at an applied load of 114 kN (26 kips) per hydraulic jack, equivalent to a uniform distributed load of 142.5 kN/m (9.8 kip/ft), which is 6.33x the nominal wall load. Note that the additional load carrying capacity of the deck slab overhang beyond the dead load of a single sound barrier is necessary to resist lateral loading. As the loading of the edge of the slab was increased, the top layer of transverse reinforcement above the outer edge of the stem yielded, followed by loss of aggregate interlock resulting in failure. The deflection of the middle of the slab directly under the loading beam when the system was loaded to ultimate capacity was 6.36 mm (0.25 in).

As a baseline, Figure 14 shows the specimen prior to testing. The markings on the top of the deck in this figure show preexisting hairline cracks in the deck.



Figure 14: Deck slab prior to experimental testing

Cracking was first observed on the top side of the deck at the 84 kN (19 kip) load per jack and were marked on the specimen in dark blue ink. The thin cracking on the top of the deck surface was discontinuous and approximately followed the two top longitudinal steel reinforcement bars adjacent to the edge of the stem wall as shown in Figure 15.

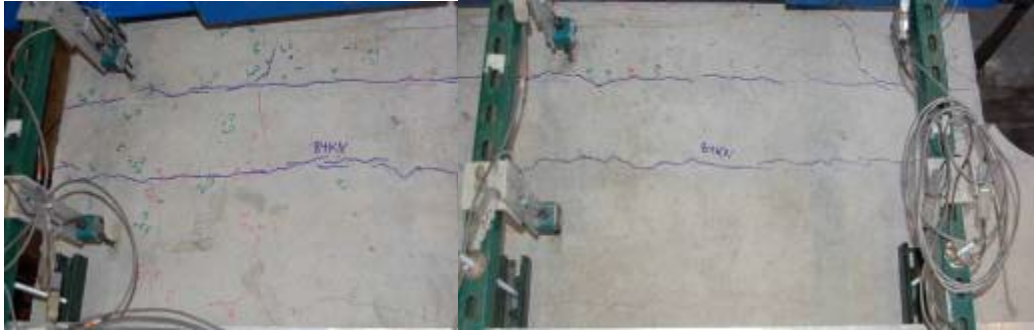


Figure 15: Initial cracking of deck slab at 84kN (19 kip) per jack- top view of deck

Minor diagonal cracks along both the central and the exterior edge of the deck slab were also observed at this load level as seen in Figure 16. Small diagonal cracks initiating on the top surface of the deck observed at each end of the specimen are shown in Figures 16(a) and (b).



(a) Detail of central edge of slab



(b) Detail of exterior edge of slab

Figure 16: Initial cracking of deck slab at 84kN (19 kip) per jack - side view of deck

Additional opening of small cracks was observed at the load level of 102 kN (23 kip) per jack and these cracks were marked with red ink as shown in Figure 17. The cracks that followed the two top longitudinal bars opened further and became continuous over the majority of the specimen. Additional cracks going across the width of the specimen formed on the top of the slab as seen in Figure 17.

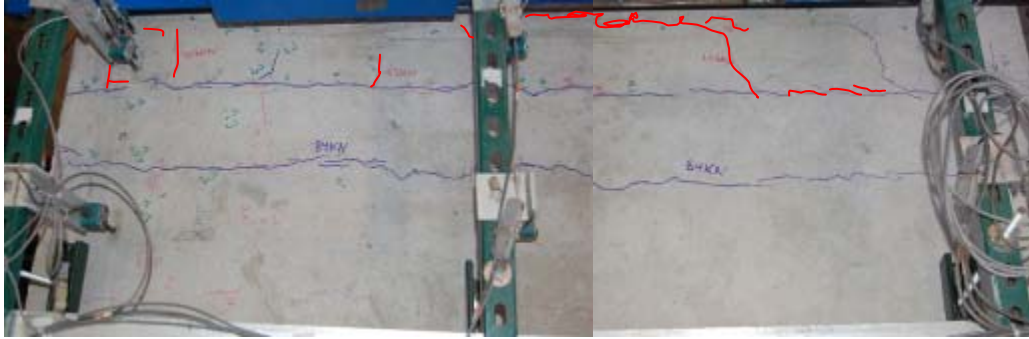


Figure 17: Crack marking of deck slab at 102 kN (23 kip) per jack- top view of deck

When the load level of 114 kN (26 kip) per jack was reached, a large diagonal crack opened and quickly propagated, which was clearly visible on the central edge of the slab as shown in Figure 18(a). This load level was determined to be the ultimate capacity of the overhang for resisting vertical loads.



(a) Central side of slab



(b) Exterior side of slab

Figure 18: Cracking observed at ultimate capacity- side view of deck

The cracking progressed rapidly along the top surface of the deck as shown in Figure 19 and the concrete adjacent to the loading beam settled several millimeters as seen in Figure 20.

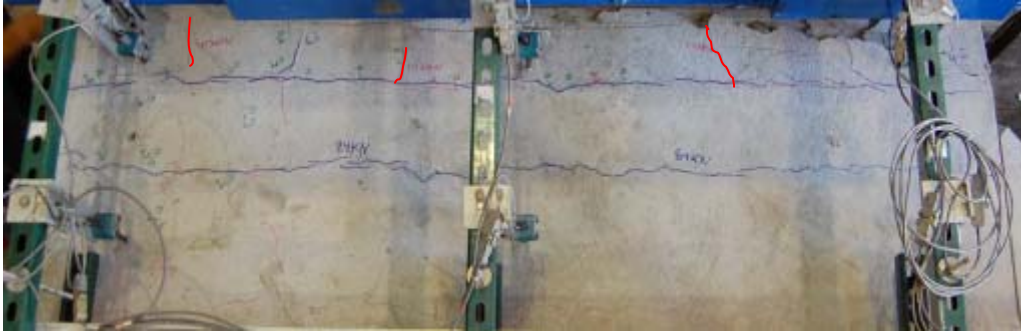


Figure 19: Cracking observed at ultimate capacity- top view deck



Figure 20: Detail of cracking at ultimate capacity in central section of deck near loading beam

After the loading of the specimen was completed, all testing equipment and instrumentation was fully removed and the observed cracks were marked in orange ink. The orange diagonal cracks on the top surface of the deck face toward the hole in the deck as shown in the upper left-hand corner of Figure 21.

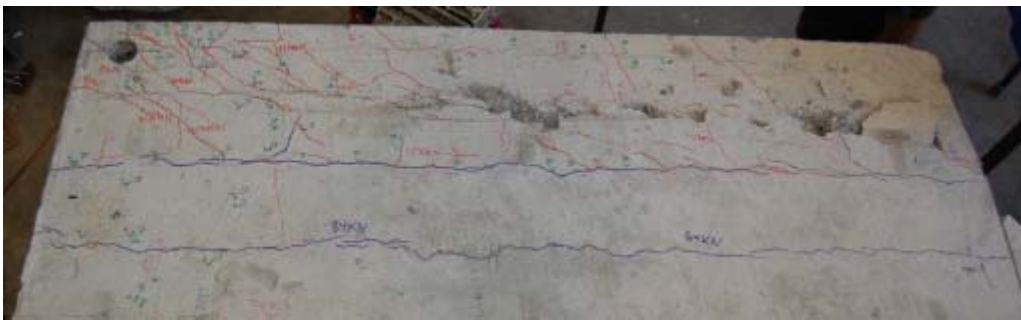


Figure 21: Cracks observed on top of slab tested to ultimate capacity

The loose concrete was then removed in order to better observe the failure surfaces as shown in Figure 22 and Figure 23. Increased damage was present on the central side of the deck as compared to the exterior side.



Figure 22: Top view of deck slab tested to ultimate capacity after removal of loose concrete

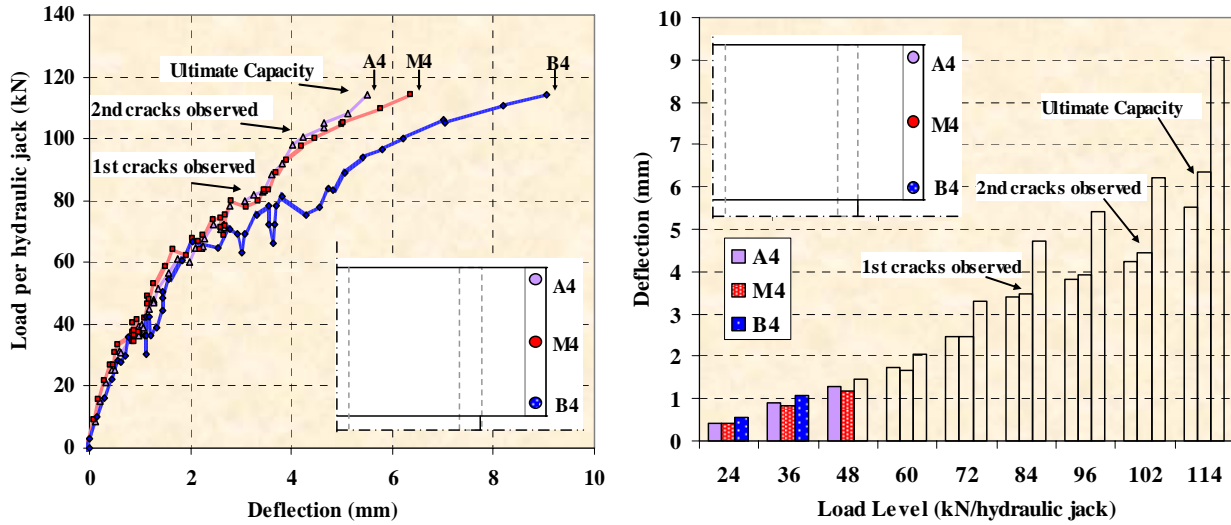
In Figure 23(b), the slight deformation in the rebar due to the yielding of the steel is observed. It is also noted that the concrete remained firmly attached beyond the longitudinal rebar.



(a) Edge of deck prior to loose concrete removal (b) After removal

Figure 23: Detail of most severely damage section

The primary variables in defining the overall structural response of the bridge deck slab are the load per hydraulic jack at which significant damage or failure occurred and the corresponding center deflection of the slab, directly below the actuator. Additional instrumentation serves to add supplementary data regarding the deformation of the specimen during testing. As observed in Figure 24, the deflection of the three linear potentiometers directly below the loading beam indicate comparable deflections for lower loading levels and higher deflections with increasing load at the central edge of the overhang, which contains linear potentiometer B4.



(a) Load versus deflection profiles (b) Comparison of linear potentiometers below loading beam

Figure 24: Comparisons of deflections at the edge of the deck slab overhang

At the load level of 84 kN (19 kips) per hydraulic jack where cracking in the deck was first observed, equivalent to a uniform distributed dead load of 105 kN/m (7.2 kip/ft) or approximately 5x the nominal wall load, linear potentiometers A4 and M4 deflected similarly while the linear potentiometer B4 exhibited a 1.3 mm (0.051 in) or 37% greater deflection value. At the load level of 102 kN (23 kip) per hydraulic jack where the 2nd set of crack marking took place, equivalent to a uniform distributed dead load of 126 kN/m (8.7 kip/ft) or nearly 6x the nominal wall load, the deflection at B4 was 2.0 mm (0.078 in) or 39% greater than the other two linear potentiometers. The difference is due to levels of cracking. The profiles along the center of the specimen (Figure 26) and at both edges (Figures 25 and 27) shown below exhibit similar deflection profiles and indicate that negligible vertical deformations occur in the deck beyond the adjacent stem wall due to edge loading of the deck slab overhang.

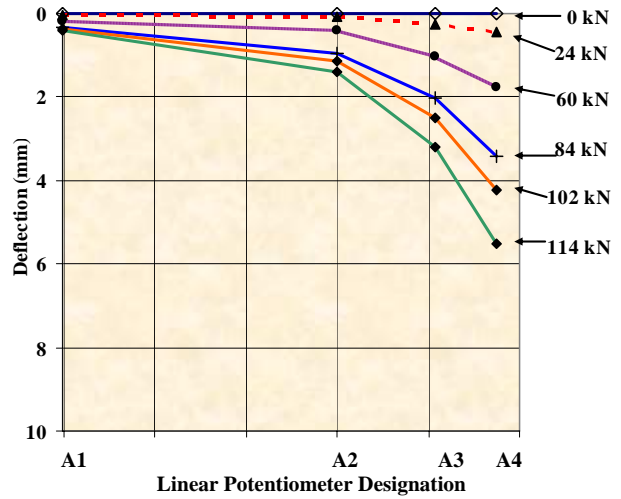
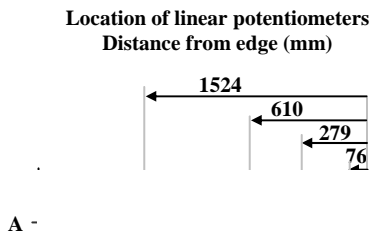


Figure 25: Deflection profile along the outer edge of specimen (Line A)

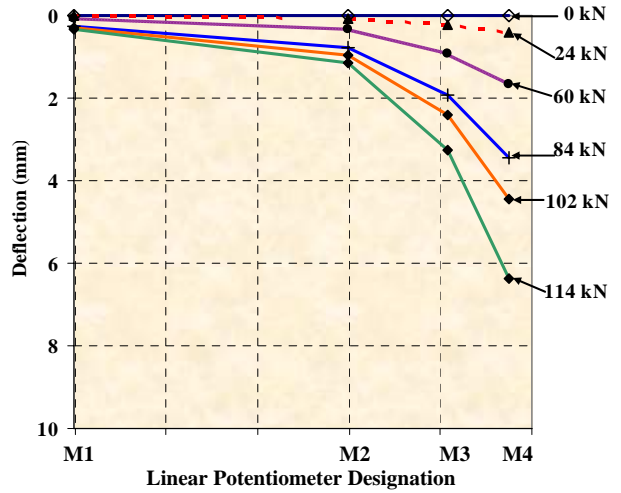
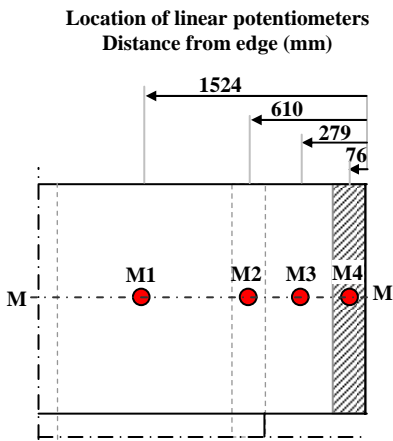


Figure 26: Deflection profile along center of specimen (Line M)

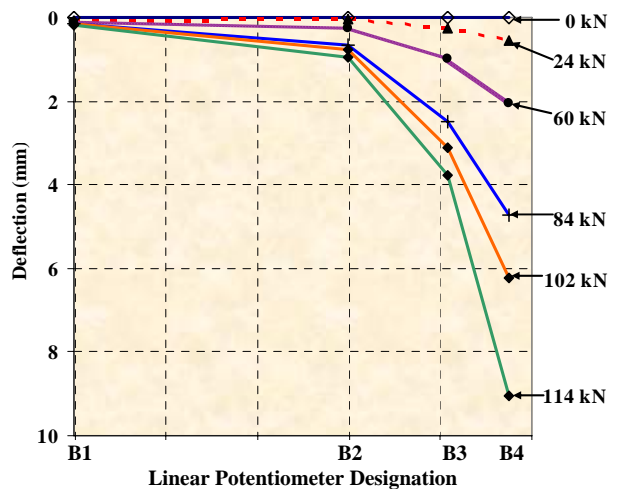
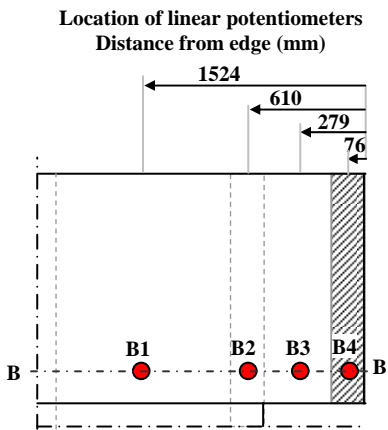


Figure 27: Deflection profile along the central edge of specimen (Line B)

The deflection profile shown in Figure 28 shows comparable deflections along the overhang at a distance midway to the adjacent stem wall. Figure 29 illustrates comparable deflections directly below the point of load application along the overhang for lower load levels with less symmetric deformations observed for higher load levels after cracking was observed throughout the specimen. Through a comparison of these figures, the results indicate a symmetric structural response for load levels prior to the initial observation of cracking in the specimen and greater deflections on one side at higher loading levels.

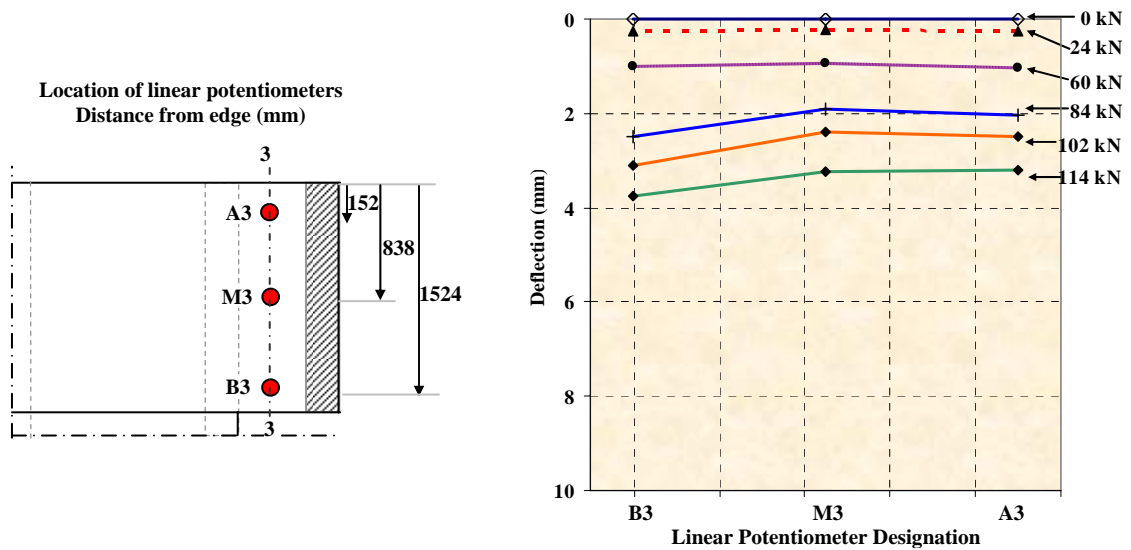


Figure 28: Deflections midway along overhang (Line 3)

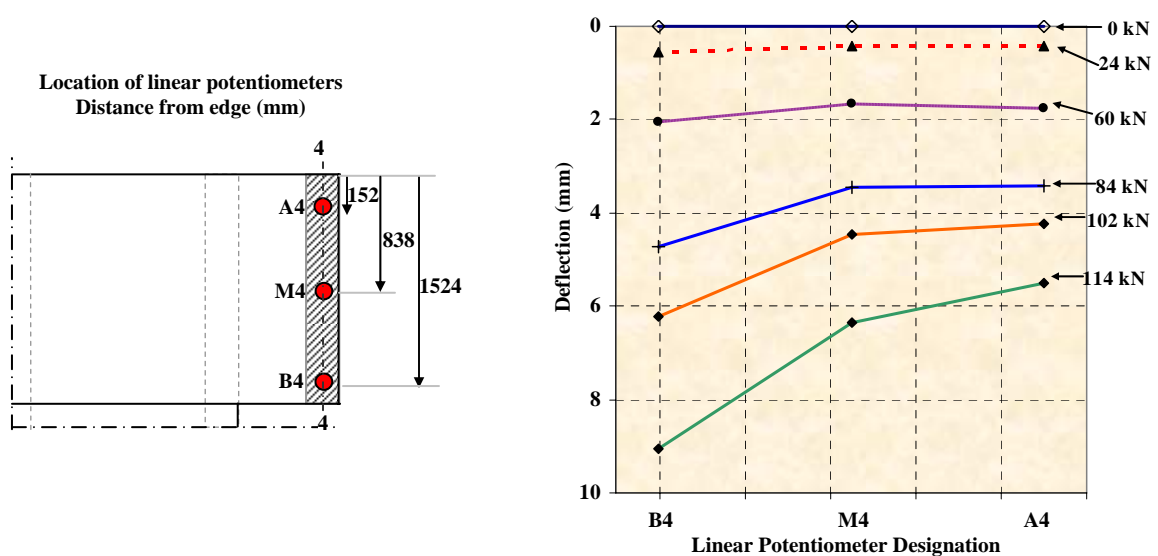


Figure 29: Deflections directly below loading beam (Line 4)

4.6 Comparison with Theory

The max moment found via moment curvature analysis of 117.2 kN-m (85.6 kip-ft) was within 6.5 % of the actual moment applied to the structure at the max loading of 114 kN (26 kip) per hydraulic jack, which corresponds to an applied moment of 110.0 kN-m (81.0 kip-ft). The moment capacity estimate of 97.0 kN-m (71.6 kip-ft), determined using the ACI 318-08 prescribed equation, was off from the experimentally determined moment capacity by 11.8%.

5. REHABILITATED TEST

The following section presents NSM FRP strengthening design options for achieving the desired capacity increase and describes the implementation, testing and analysis of the chosen rehabilitation design.

5.1 Calculations for Potential CFRP NSM Strengthening Schemes

The increased moment demand on the test specimen's deck slab due to the addition of the soundwall is calculated and this value is used as the basis for determining the desired capacity increase. The corresponding total area of NSM CFRP needed to achieve the desired moment capacity increase is calculated and design options for five different available CFRP reinforcement products are presented.

The dead weight of a typical sound wall used for bridges in California was calculated from the Caltrans' concrete masonry soundwall design on bridges [20]. Using this design with normal weight concrete, the gravity load per unit length for the soundwall was determined to be 13.5 kN/m (0.92 kip/ft). Note that the weight of the traffic barrier is not included as part of the increased moment demand calculation because it is assumed that the weight of the traffic barrier was already accounted for in the original design of the deck slab overhang. The tested section of overhang was 1600 mm (5 ft 6 in) long therefore the total load applied to the specimen from the soundwall is 22.6 kN (5.08 kip). The equivalent moment applied to the structure due to this dead load can be obtained by multiplying the total load applied by the distance between the applied load and the edge of the stem, also known as the moment arm. The equivalent additional moment demand due to the soundwall was found to be 10.91 kN-m (8.05 kip-ft).

A successful repair would strengthen the overhang to accommodate this increased moment demand with a reasonable safety margin. For initial calculation purposes, a safety margin of 3 was deemed appropriate.

$$M_{demand_increase} = M_{wall} \cdot 3 \quad (6)$$

This translates to an increase in moment demand of 32.7 kN-m (24.1 kip-ft). Therefore, the NSM flexural strengthening will be designed to increase the capacity of the overhang by at least this value. The experimentally determined moment capacity of the as-built reinforced concrete deck slab overhang without FRP was found to be 110 kN-m (81 kip-ft). Therefore, the new moment capacity after strengthening should be at least 142.7 kN-m (105.1 kip-ft), which corresponds to a minimum required moment capacity increase of 29.7 percent over the capacity of the as-built specimen without FRP.

The increased moment capacity due to FRP strengthening is equal to the sum of the contribution from the tension steel (compression steel is ignored for this calculation) and the contribution from the FRP reinforcement:

$$M_{n_strengthened} = A_s f_y \left(d - \frac{a}{2} \right) + \Psi_f \cdot A_f f_{fe} \cdot \left(d_f - \frac{a}{2} \right) \quad (8)$$

The definitions of the variables in the above equation are shown below.

Steel properties:

A_s = Total area of tension steel in slab overhang test specimen

f_s = Experimentally determined yield strength of steel reinforcement

d = Distance to centroid of tensile steel reinforcement

a = Depth of concrete compression block, assuming rectangular stress distribution

FRP properties:

Ψ_f = Additional reduction factor recommended by ACI 440.2R (Section 9.6.1) [12]

d_f = Distance from the compression fiber to the centroid of the FRP

f_{fe} = $E_f \cdot \epsilon_{fe}$ Effective stress in the FRP assuming elastic behavior

E_f = Experimentally determined modulus of elasticity of FRP

ϵ_{fe} = Effective strain in FRP reinforcement

By rearranging equation 8, an expression for the area of FRP reinforcement required in order to achieve a specified moment capacity increased can be obtained:

$$A_{f_required} = \frac{M_{n_strengthened} - A_s f_y \left(d - \frac{a}{2} \right)}{\psi_f \cdot f_{fe} \cdot \left(d_f - \frac{a}{2} \right)} \quad (9)$$

The required area of FRP obtained from this expression can be used to evaluate the feasibility of different FRP strengthening options. Note that the area of FRP required is the total area needed for the specimen overhang and thus must be distributed along the width of the slab overhang.

5.2 Options for Rehabilitation

The seven product options evaluated for this rehabilitation design were different sizes of SIKA's pultruded carbon fiber CarboDur rods and strips as well as Hughes Brothers' pultruded carbon fiber Aslan 500 rectangular rods. The physical characteristics of each option are provided in Table 2 for reference.

Product Type	Source	Product Designation	Diameter		Thickness		Width		Area		Tensile Modulus	
			mm	in	mm	in	mm	in	mm ²	in ²	GPa	Msi
Rod	SIKA	¼ in. dia.	6.35	0.25					1.27	0.05	155	22.5
Rod	SIKA	3/8 in dia.	9.53	0.375					2.79	0.11	155	22.5
Strip	SIKA	S512			1.2	0.047	50	1.97	60	0.093	165	23.9
Strip	SIKA	S812			1.2	0.047	80	3.15	96	0.149	165	23.9
Strip	SIKA	S1012			1.2	0.047	100	3.94	120	0.186	165	23.9
Bar	Hughes Brothers	#2			2	0.079	16	0.63	31.2	0.049	124	18
Bar	Hughes Brothers	#3			4.5	0.177	16	0.63	71.3	0.110	124	18

Table 2: Physical properties of pultruded CFRP strengthening product options [21,22,23]

The number of reinforcements required to attain the desired moment capacity increase was calculated for each of the seven potential options using calculations described in the previous section (Equation 9) and the results are shown in Table 3. For calculation of the effective stress in the FRP, ε_{fe} , a strain of 0.65% was assumed based on design recommendations for FRP post-strengthening of reinforced concrete slabs [24, 25]. The tensile modulus for each of the different FRP reinforcement options was obtained from manufacturer reported data. Since the FRP reinforcement type had not been selected yet, the distance from the compression fiber to the centroid of the FRP, d_f , was assumed to be the full depth of the slab. Note that this assumption will slightly overestimate the moment capacity contribution from the FRP because for NSMR applications, the reinforcement is located slightly below the surface of the structure. Assuming that the centroid of the FRP reinforcement is below the surface of the structure by a distance of between 2 mm (0.079 in) and 10 mm (0.393 in) the calculations would have overestimated the moment capacity increase due to the FRP reinforcement by between 1% and 6%.

Spacing requirements were also considered in the calculations performed for each FRP strengthening option. The maximum spacing recommendations provided by the manufacturer [26] state that on center spacing should be limited to no more than the lesser of 0.2 times the span length (L) or five times the slab thickness (h):

$$s_{limit} = \min(0.2L, 5h) \quad (10)$$

Note that the span for cantilever is taken as twice the distance to the support. This spacing limit yields a maximum recommended spacing of 203 mm (8 in). Table 3 below shows the number of units needed as well as the theoretical moment capacity increase for each type of CFRP reinforcement. As observed in the Table 3, spacing limitations govern rather than actual strength requirement limitations. Since all seven of the design options are able to achieve the increased capacity requirements, other aspects such as cost and constructability are now used to select the FRP reinforcement system.

One notable difference between the installation of CFRP strips as opposed to rods is the required depth of grooves cut into the deck. The 6.4 mm (1/4 in) diameter rods require 12.7 mm (1/2 in)

deep slots and the 9.5 mm (3/8 in) rods require 15.9 mm (5/8 in) deep rods, while the strips only require a 4 mm (0.16 in) deep groove. From a construction viewpoint, strips as opposed to rods are far easier to implement due to required groove depth. Given that there is often less cover on the top of a slab than would be required cutting deeper grooves is hazardous in that the cuts could easily cut through existing steel reinforcing bars. Thus having shallower grooves is preferred in Europe based on extensive field use.

The lower modulus of the CFRP tape of 124 GPa (18.0 Msi) versus that of the CFRP strips, 165 GPa (23.9 Msi), resulted in appreciably greater material usage for comparable strengthening schemes. As a comparison, the S512 CFRP strip has an estimated moment capacity increase of 81%, whereas the #3 size CFRP tape has an estimated moment capacity increase of only 71 % and requires an additional 19% of material above that used for the strip to achieve this increase.

Based on guidelines, material cost considerations, the CarboDur strips were recommended for use to Caltrans. On receipt of approval from Caltrans to use this option, experimental work was initiated using the flat option. Because the smallest size strip far exceeded the required moment capacity, the CarboDur S512 strips were selected, which have a 50 mm (2 in) width. The spacing was set at 203 mm (8 in) on center for the width of the test specimen such that nine total CFRP strips were used. The bars were extended past the point of inflection to achieve a necessary development length of 300 mm (11.8 in).

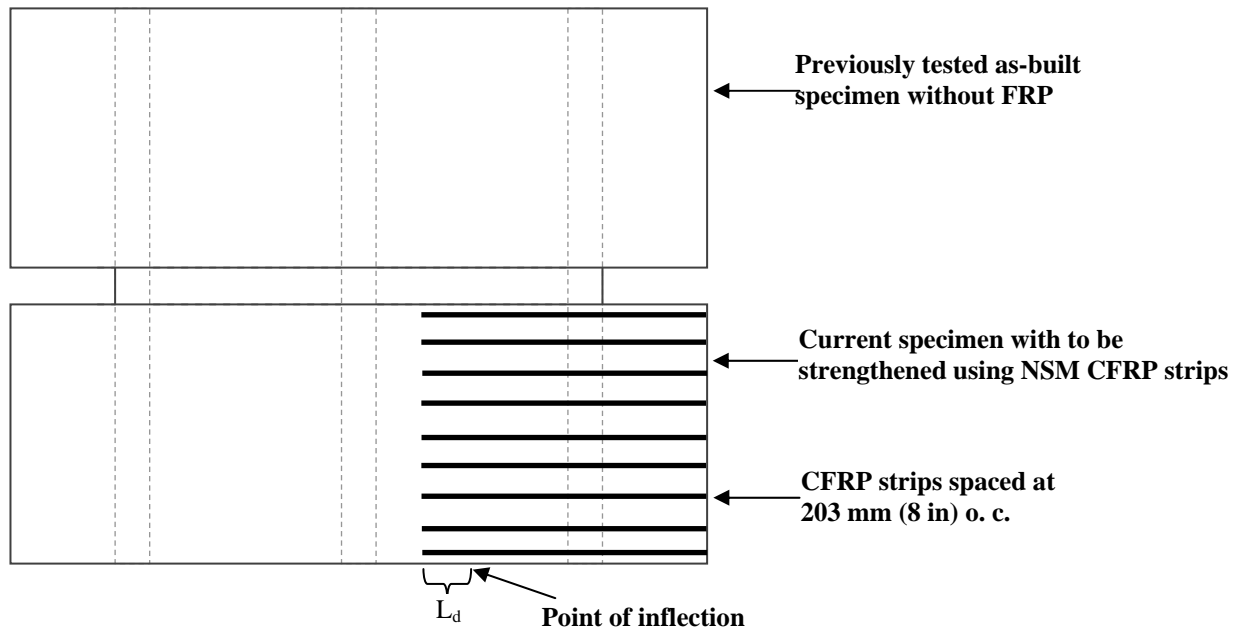


Figure 30: Plan view of deck illustrating chosen CFRP strengthening scheme

Reinforcement type	Product (Name and size)	Cross-sectional Area		# of units needed (rounded up)	Spacing w/o considering spacing limits		Spacing used (considering spacing limits)		Actual # of units (rounded up)	Total area of FRP used		Theoretical moment capacity		Moment capacity increase %
		(mm ²)	(in ²)		(mm)	(in)	(mm)	(in)		(mm ²)	(in ²)	(kN-m)	(kip-ft)	
Rod	1/4" diameter	32	0.05	7	254	10	102	4	9	226	0.45	140.7	103.7	28%
Rod	3/8" diameter	71	0.11	4	432	17	203	8	9	639	0.99	191.8	141.5	74%
Strip	S512-50mm width	60	0.093	4	432	17	203	8	9	540	0.84	182.4	134.5	66%
Strip	S812-80mm width	96	0.149	3	559	22	203	8	9	865	1.34	233.2	172.0	112%
Strip	S1012-100mm width	120	0.186	2	838	33	203	8	9	1080	1.67	256.6	189.2	133%
Tape	#2	31	0.049	9	203	8	203	8	9	281	0.44	131.5	96.9	20%
Tape	#3	71	0.11	4	432	17	203	8	9	642	0.99	173.1	127.6	57%

Table 3: Calculation table using different FRP strengthening options

5.3 Rehabilitation Construction

The following section details the implementation of the NSMR strengthening scheme chosen in Section 5.2. Nine (9) rectangular grooves spaced at 203 mm (8 in) o.c. were cut in the top deck of the test specimen with dimensional tolerances of 70 mm - 76 mm (2 ¾ in - 3 in) for the width and 6 mm - 13 mm (¼ in to ½ in) for depth. The grooves were each 2.74 m (8 ft) long and the cut grooves are shown in Figure 31.



Figure 31: Grooves cut in deck for NSM strengthening

After the grooves were cut to the proper dimensions, the surface was roughened to achieve the minimum required concrete surface profile (CSP) of 3 as defined by the ICRI surface profile guidelines [27].

The CarboDur S 512 carbon fiber laminate strips were cut to length and the top and bottom surfaces were wiped clean using methyl ethyl ketone (MEK) to remove all residual carbon dust from the surface prior to the installation of strain gages on the top surface of the strips. An additional cleaning with MEK was performed immediately prior to installation of the strips into the test specimen to remove any remaining contaminants and surface oxidization. A high-modulus, high-strength, structural epoxy paste known as SikaDur 30 was used for bonding the CFRP strips to the concrete. The structural properties of the CarboDur S 512 strips and SikaDur 30 resin system were experimentally determined through material characterizations performed at the University of California, San Diego within the authors' research group and these properties are shown below from [28].

Tensile Properties (ASTM D-638)	SikaDur 30	
	Mean	Standard Deviation
7 day Tensile Strength	25.29 MPa (3.671 ksi)	2.54 MPa (0.369 ksi)
Modulus of Elasticity	6.93 GPa (1.006 Msi)	0.48 GPa (0.0697 Msi)

Table 4: Tensile properties of SikaDur 30 resin system [28]

Tensile Properties (ASTM D-3039)	CarboDur S 512	
	Mean	Standard Deviation
Ultimate Tensile Strength	2,505 MPa (363.6 ksi)	82.85 MPa (12.0 ksi)
Ultimate Tensile Modulus	138.1 GPa (20.05 Msi)	5.22 GPa (0.76 Msi)
Ultimate Tensile Strain	1.580 %	0.084 %

Table 5: Tensile properties of Sika CarboDur S512 CFRP strips [28]

After the SikaDur 30 resin system was thoroughly mixed, the neat resin was applied to each groove as a primer using a spatula to form a uniform thickness of 1.6 mm (1/16 in) as shown in Figure 32. A specialized applicator was also used to apply a precisely controlled thickness of resin onto each of the carbon fiber strips and the strips were carefully placed in the grooves.



Figure 32: Application of resin system used in grooves to bond CFRP strips to concrete

A rubber roller was then used to properly seat each strip, using adequate pressure to force SikaDur 30 gel out on both sides of the laminate so that the bond line between the concrete and

FRP strip does not exceed 3 mm (1/8 in) [29]. Excess gel was carefully removed and the installed strips are shown in Figure 33.



Figure 33: CFRP strips installed

After the resin system had cured for 24 hours, a low viscosity resin system, which was used for the wear surface applied to the top of the FRP strips, was poured over the top of the strips up to the level of the original concrete deck. The top layer of resin was mixed with sand to allow for improved thermal compatibility with the surrounding concrete and to provide a non-skid wear surface for the top of the deck. After the installation of the NSM CFRP strengthening scheme was completed, the instrumentation was installed and the specimen was ready for testing to determine the effectiveness of the repair.

In order to monitor the curing of the CarboDur 30 resin system used to attach the CFRP strips to the deck slab, small test samples were made using resin mixed for installation of the strips and the samples were placed adjacent to the test specimen to ensure comparable curing conditions. These resin samples were tested daily for a period of seven days using both dynamic mechanical thermal analysis (DMTA) and differential scanning calorimetry (DSC) techniques. The results obtained from these experiments regarding the glass transition temperature, T_g , of the resin system are shown in Table 6. The trends from the glass transition temperature data over time shown below indicate that the SikaDur 30 resin system achieved nearly full cure after approximately 4-5 days.

Time	DMTA T _g results	DSC T _g results
	°C	°C
Day 1	57.13	37.50
Day 2	59.15	38.50
Day 3	---	---
Day 4	64.39	41.50
Day 5	62.26	42.25
Day 6	64.26	43.00
Day 7	63.61	43.00

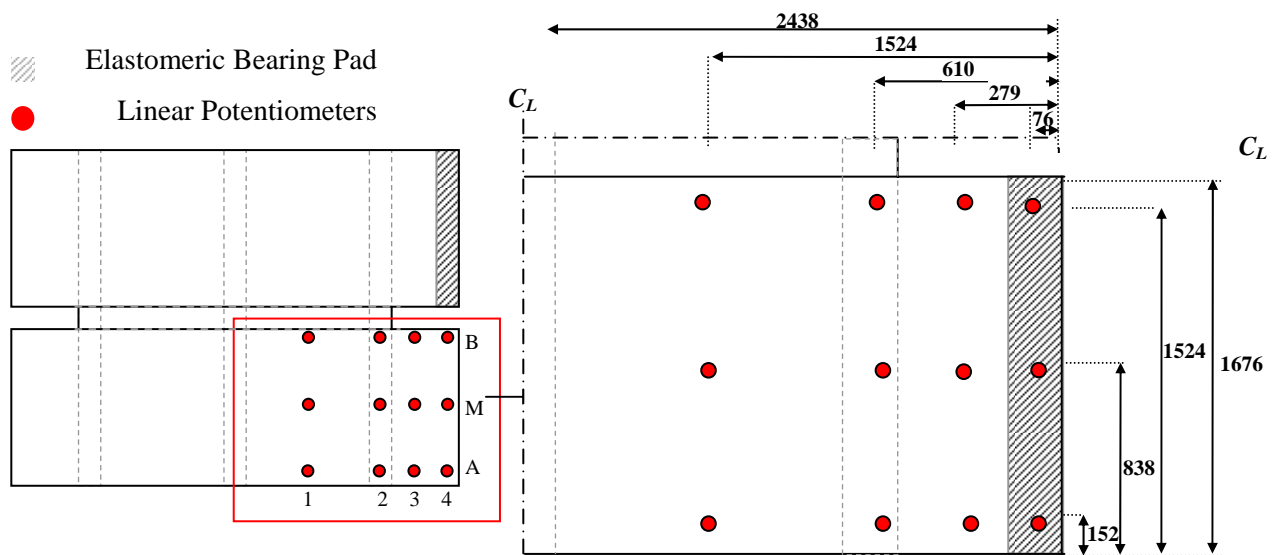
Table 6: T_g progression of CarboDur 30 resin used in NSMR installation

5.4 Capacity Calculations

Following the implementation of the chosen NSM CFRP strip rehabilitation scheme, theoretical predictions for capacity were recalculated using the experimentally determined material properties given in Table 6 along with an assumed CFRP strip embedment depth of 3 mm (1/8 in) and reduced FRP strain capacity of 0.65% as described in Section 5.1. The increased moment capacity calculation due to FRP strengthening described in Section 5.1 yields a theoretical moment capacity of 167.3 kN-m (123.4 kip-ft), which corresponds to a 52% increase in moment capacity over the experimentally determined value for the as-built specimen. The moment curvature analysis performed on the FRP rehabilitated specimen yielded a moment capacity of 185.5 kN-m (136.4 kip-ft), which corresponds to a 69 % increase in load carrying capacity over the as-built specimen.

5.5 Instrumentation

The total instrumentation for this experiment consisted of 16 linear potentiometers, 47 strain gages and 2 load cells. One central row and two outer rows, each with four linear potentiometers were used to measure the vertical deflection of the deck slab. The four linear potentiometers within each row were positioned at the midspan of the adjacent cell, above the adjacent stem, in between the stem and the loading beam, and directly below the loading beam, as shown in Figures 11(a) and (b).



(a) Plan view of specimen

(b) Section of deck slab with linear potentiometer details

Figure 34: Position of linear potentiometers for measuring deflections of deck slab

The deflection of the elastomeric bearing pad was measured using four linear potentiometers, with one linear potentiometer at each corner of the loading beam using the same layout as the as-built specimen shown in Figure 12.

All 47 strain gages were applied to the top side of the nine pultruded CFRP strips, parallel to the direction of the fibers as shown in Figure 33. The two strain gage layout patterns used on this specimen, illustrated in Figure 35, were applied to alternating CFRP strips throughout the width of the specimen as shown in Figure 36.

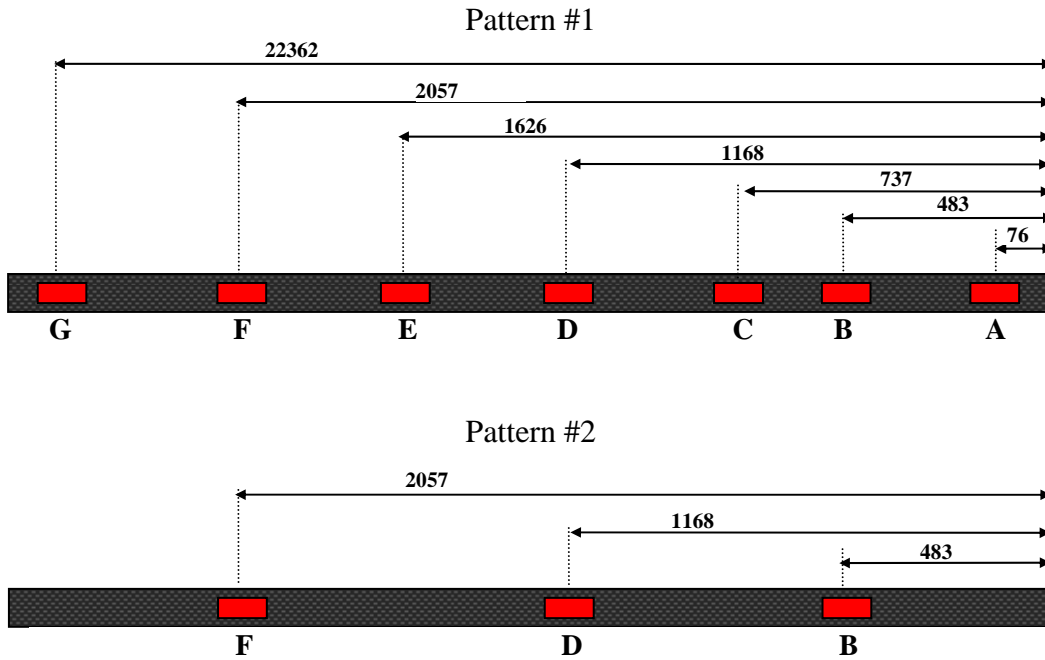


Figure 35: Strain gage patterns and designations

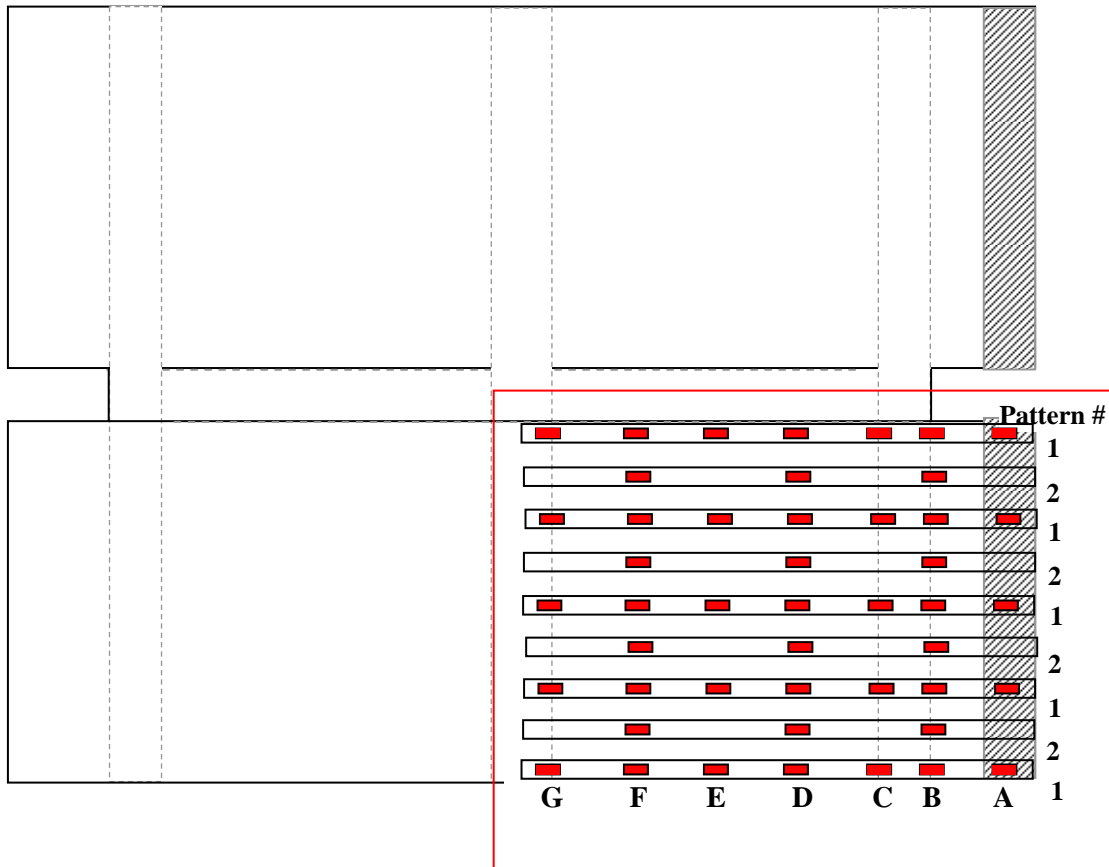


Figure 36: Position of strain gages attached to CFRP strips

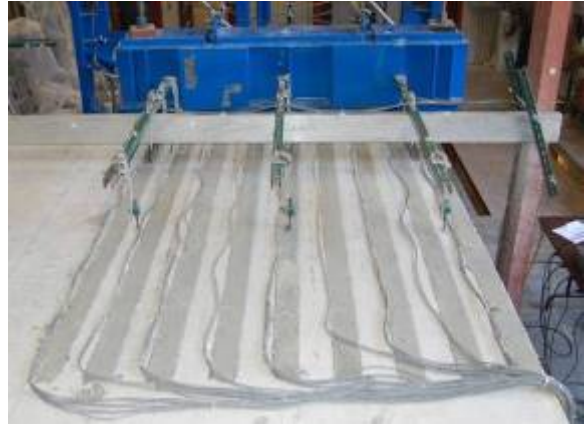


Figure 37: Completed installation of CFRP strips with full instrumentation setup

5.6 Loading Protocol

The overhang of the deck slab was loaded using the test setup shown in Figure 7 and described in Section 3.1 by incrementally increasing the hydraulic pressure supplied to the two hydraulic jacks. Adequate time was taken between loading levels to ensure that the hydraulic pressure had stabilized and the pressure had equalized as much as possible between the two jacks. The load applied to the deck slab was monotonically increased following the loading sequence shown in Table 7. The load was held briefly at each load level so that observations could be made.

Loading step	Load per hydraulic jack		Equivalent uniform distributed load		Load Level	Notes
	(kN)	(kip)	(kN/m)	(kip/ft)		
1	24	5	30.0	2.1	---	Initial load
2	36	8	45.0	3.1	2x wall load	---
3	48	11	60.0	4.1	---	---
4	60	13	75.0	5.1	---	---
5	72	16	90.0	6.2	4x wall load	---
6	84	19	105.0	7.2	1 st set of cracks observed for as-built specimen	---
7	90	20	112.5	7.7	5x wall load	---
9	101	23	126.3	8.7	Calc'd moment capacity as-built specimen	---
10	114	26	142.5	9.8	Ultimate capacity as-built specimen	---
11	116	26	145.0	9.9	Calc'd shear capacity as-built specimen	1st set of cracks observed
12	130	29	162.5	11.1	---	---
13	136	31	170.0	11.6	---	2nd set of cracks observed
14	142	32	177.5	12.2	~8x wall load	---
15	148	33	185.0	12.7	---	---
16	160	36	200.0	13.7	~9x wall load	3rd set of cracks observed
17	166	37	207.5	14.2	---	---
18	172	39	215.0	14.7	---	---
19	178	40	222.5	15.2	~10x wall load	---
20	184	41	230.0	15.8	---	4th set of cracks observed
21	190	43	237.5	16.3	---	---
22	196	44	245.0	16.8	~11x wall load	Ultimate Capacity

Table 7: Loading protocol used for FRP rehabilitated specimen

5.7 Experimental Results

The ultimate capacity of the FRP rehabilitated deck slab was reached at an applied load of 196 kN (44 kips) per hydraulic jack, equivalent to a uniform distributed load of 245 kN/m (16.8 kip/ft), which is 11 x the nominal soundwall load. At this load level, the deflection of the middle of the slab under the loading beam was 8.73 mm (0.34 in). The maximum strain value achieved in the CFRP strips at ultimate capacity was 3846 microstrains. At the ultimate capacity of the specimen, debonding of the FRP from the concrete occurred due to a tensile failure of the concrete cover layer located between the FRP and the top layer of rebar. This loss of compatibility within the section was quickly followed by the opening and propagation of a large diagonal crack along the compression strut formed with the adjacent stem wall.

Cracking was observed and marked on the specimen at the four load levels of 116 kN (26 kip), 136 kN (31 kip), 160 kN (36 kip) and 184 kN (41 kip) per hydraulic jack. The extent of visible cracking on the top and sides of the deck of the FRP rehabilitated specimen shown in Figure 38 and Figure 39 occurred at the load level of 184 kN (41 kip) per hydraulic jack, which was over twice the load at which comparable cracking was observed on the as-built specimen. The comparable initial cracking observed on the as-built specimen, which was described in section 4.5, occurred at a load level of 84 kN (19 kip) per hydraulic jack and is shown in Figure 15 and Figure 16 on page 19. The thin cracking on the top of the deck surface that occurred in the FRP rehabilitated specimen observed at the load level of 184 kN (41 kip) per hydraulic jack was discontinuous and approximately followed the top longitudinal steel reinforcement bars adjacent to the edge of the stem wall as shown in Figure 38.



Figure 38: Cracking of deck slab at 184 kN (41 kip) per jack- top view of deck

Minor diagonal cracks along both the edges of the slab, which initiated from the top surface of the deck, are shown in Figure 39.



(a) Detail of central edge of slab



(b) Detail of exterior edge of slab

Figure 39: Cracking of deck slab at 184 kN (41kip) per jack - side view of deck

When the load level of 196 kN (44 kips) per hydraulic jack was reached, the ultimate tensile strength of the top concrete cover layer was exceeded and the bond between the FRP and the concrete was lost. This damage was quickly followed by the opening and propagation of a large diagonal crack along the compression strut formed with the adjacent stem wall shown in Figure 40. This load level was determined to be the ultimate capacity of the overhang for resisting vertical loads.



(a) Central side of slab



(b) Exterior side of slab

Figure 40: Cracking observed at ultimate capacity- side view of deck

The top surface of the deck slab after failure of the specimen can be observed in Figure 41 and the cracking due to the interfacial failure between the FRP strips and the concrete can be observed in the in the upper left hand corner of Figure 41, adjacent to the loading beam.



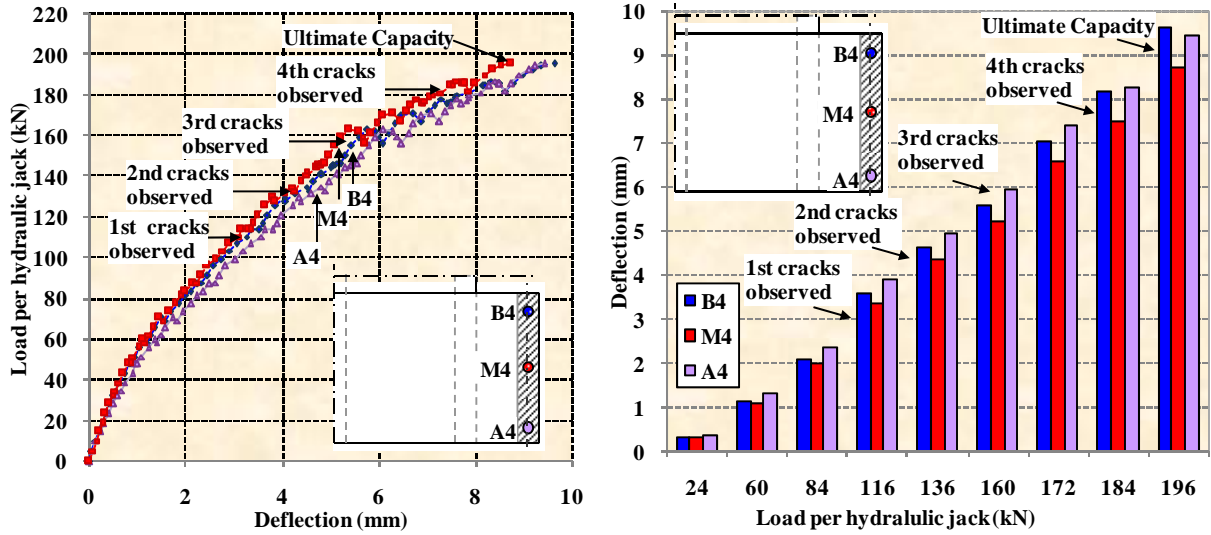
Figure 41: Cracking of deck slab at ultimate capacity- top view of deck

After the loading of the specimen was completed, all testing equipment and instrumentation was fully removed to allow for easier observation of the damage present on the specimen. Figure 42 shows the top view of the deck at ultimate capacity. Any loose concrete was removed in order to better observe the failure surfaces, however unlike the as-built specimen in which significant loose concrete was removed after it was tested, nearly all of the concrete remained attached to the tested FRP rehabilitated specimen, despite the interfacial failure that occurred between the FRP and the concrete. Note that the debonding of the CFRP strips from the concrete occurred adjacent to where the tensile stresses on the top of the deck are maximum while the CFRP strips remained attached for the majority of the of the slab overhang.



Figure 42: Side view of tested FRP rehabilitated specimen after removal of loose concrete

As observed in Figure 43, the three linear potentiometers directly below the loading beam maintained comparable deflections throughout the loading range applied to the test specimen. At the failure load for the specimen, the deflections of these three linear potentiometers were within 10% of each other which corresponds to less than 1 mm (0.04 in) difference in deflection values.



(a) Load versus deflection profiles (b) Comparison of linear potentiometers below loading beam

Figure 43: Comparisons of deflections at the edge of the deck slab overhang

The profiles along the center of the specimen (Figure 45) and at both edges (Figure 44 and Figure 46) shown below exhibit similar deflection profiles throughout the loading range.

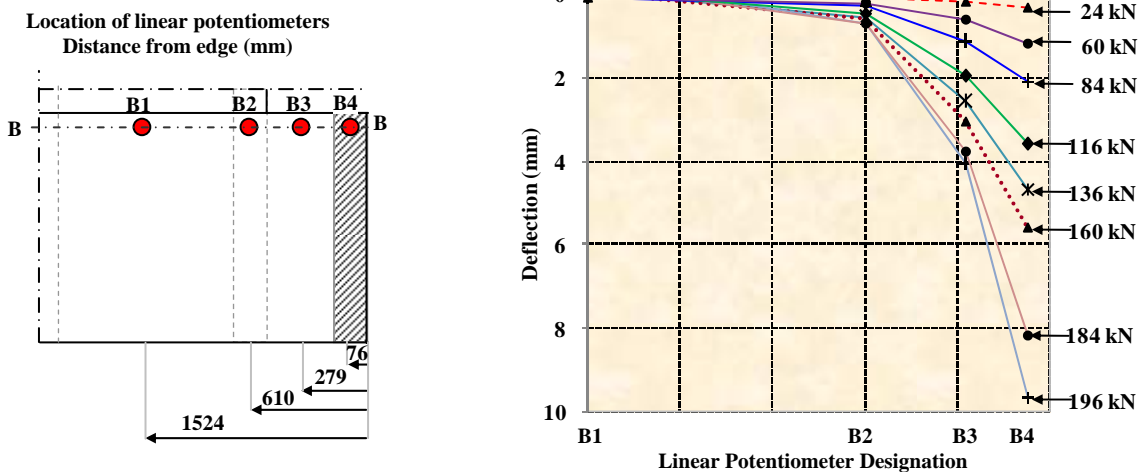


Figure 44: Deflection profile along the central edge of specimen (Line B)

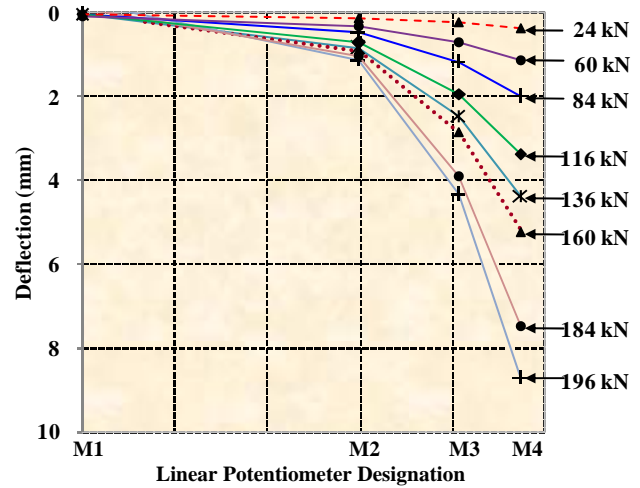
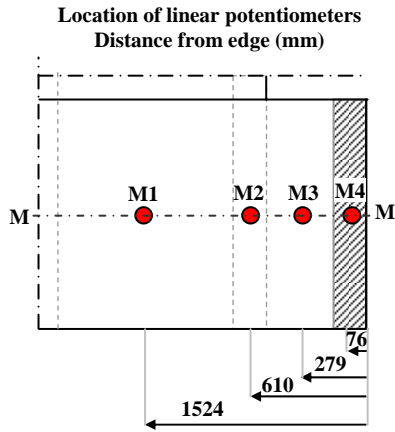


Figure 45: Deflection profile along center of specimen (Line M)

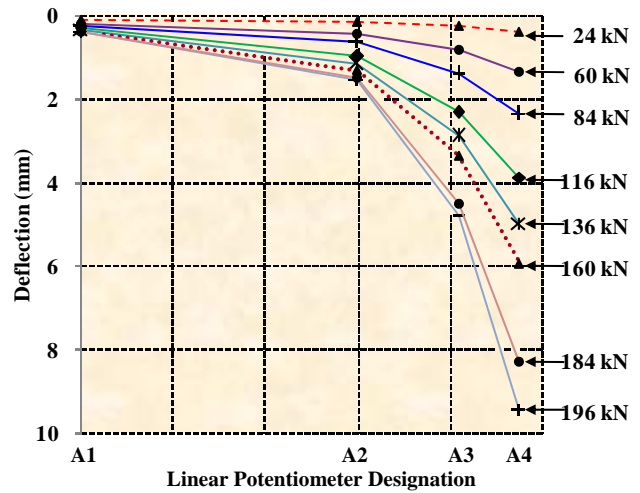
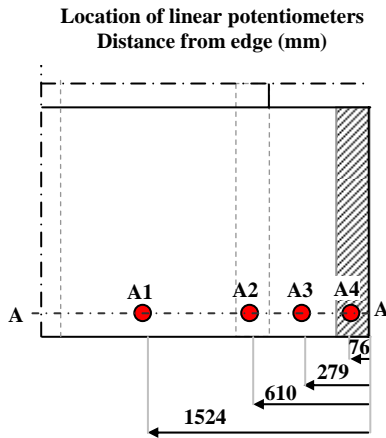


Figure 46: Deflection profile along the outer edge of specimen (Line A)

The deflection profiles shown in Figure 47 and Figure 48 also indicate comparable deflections along the overhang at a distance midway to the adjacent stem wall and directly below the point of load application respectively.

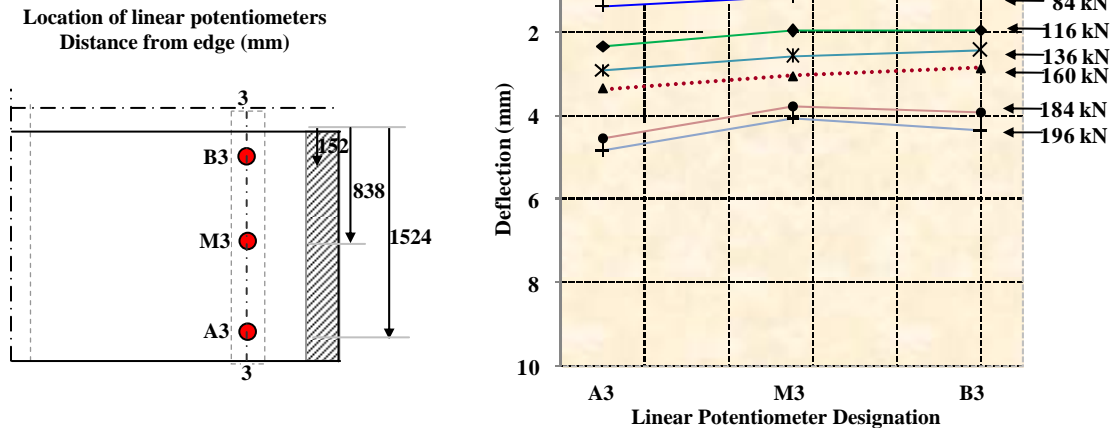


Figure 47: Deflections midway along overhang (Line 3)

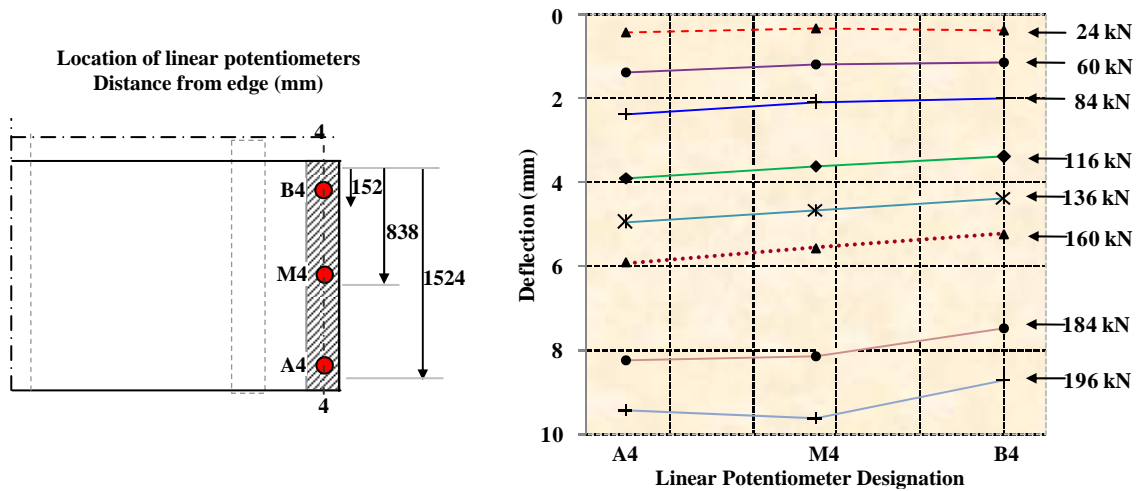


Figure 48: Deflections directly below loading beam (Line 4)

The strains in the FRP strips are also examined throughout the NSM CFRP rehabilitated specimen. The strain profiles along the edges and the middle of the specimen are shown in Figure 49, Figure 50, and Figure 51 respectively. These strain profiles indicate that the maximum strain in the CFRP strips occurs directly above the edge of the stem wall adjacent to the deck slab overhang, referred to with the designation, “line B”. At ultimate capacity, the maximum strain in the specimen of 3846 microstrains occurs in strain gage 4B, which is located in line B near the middle of the specimen overhang.

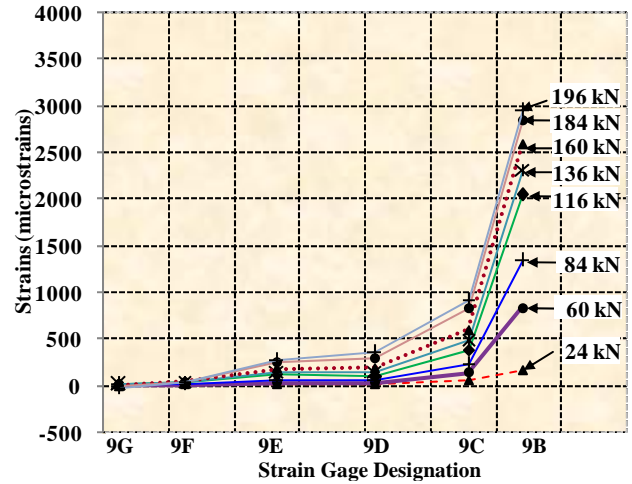
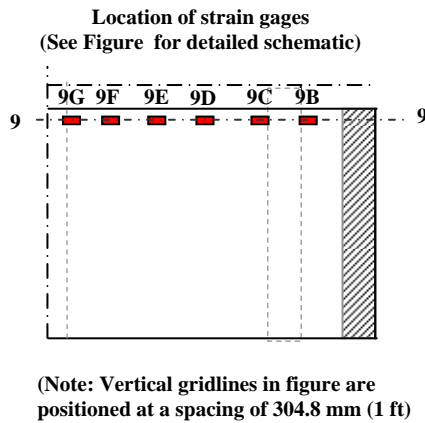


Figure 49: Strain profile along the central edge of specimen (Line 9)

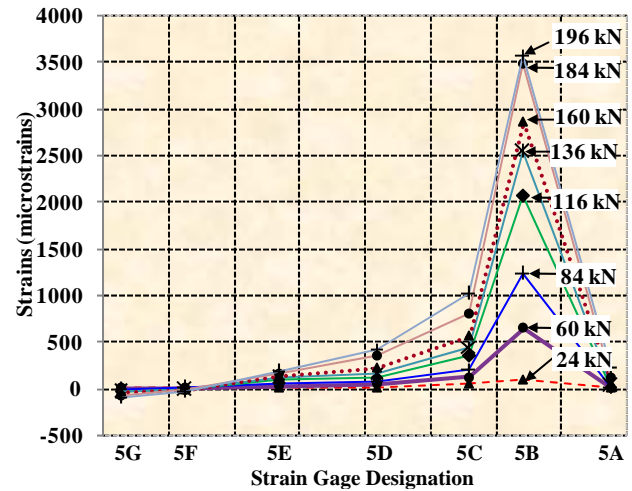
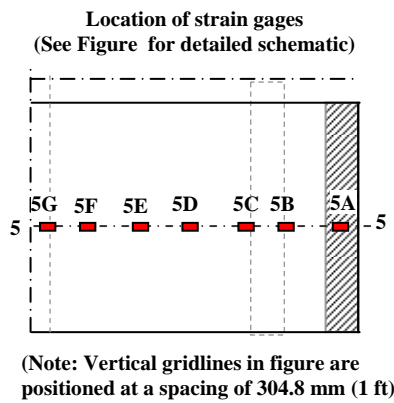


Figure 50: Strain profile along the middle of specimen (Line 5)

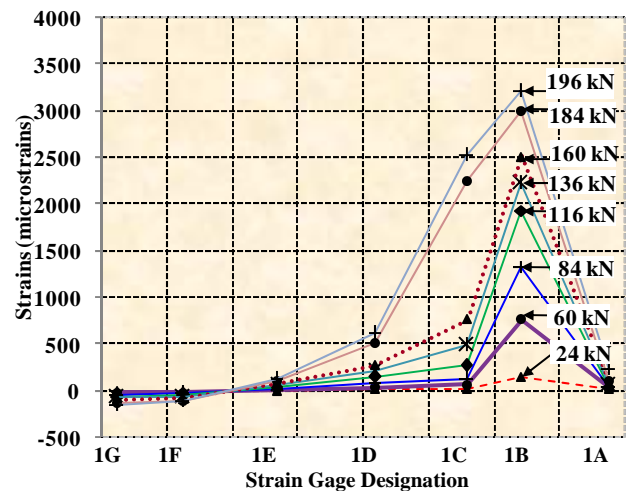
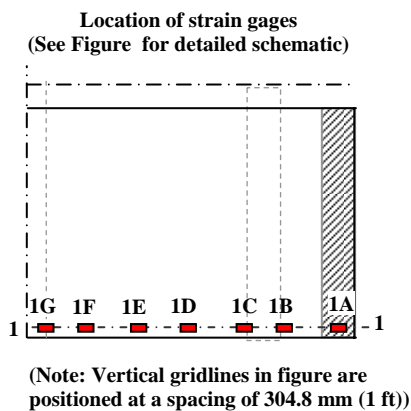


Figure 51: Strain profile along the outer edge of specimen (Line 1)

The strains drop off sharply for distances further away from the end of the overhang, with the majority of the strain gages on the opposite side of the stem wall (line C) exhibiting less than a third of the strain values shown in line B. The sharp drop in strain values at distances away from the adjacent stem wall and the insignificant strains within these regions indicate that the significantly shorter lengths of CFRP strips could be used to optimize material usage and improve constructability without affecting load transfer and the overall system response.

The strains along line B, the location where the maximum strains occur in the specimen is shown in Figure 52. This figure indicates that the distribution of strains was even along the specimen until the load level of 116 kN (26 kip) per jack was reached. At this level, cracking was first observed on the specimen and higher loading levels showed comparable but slightly less uniform strains along the specimen. The average strain along line B in the specimen at ultimate capacity was 3423 microstrains, whereas the minimum and maximum strains along line B were 2943 microstrains and 3846 microstrains respectively.

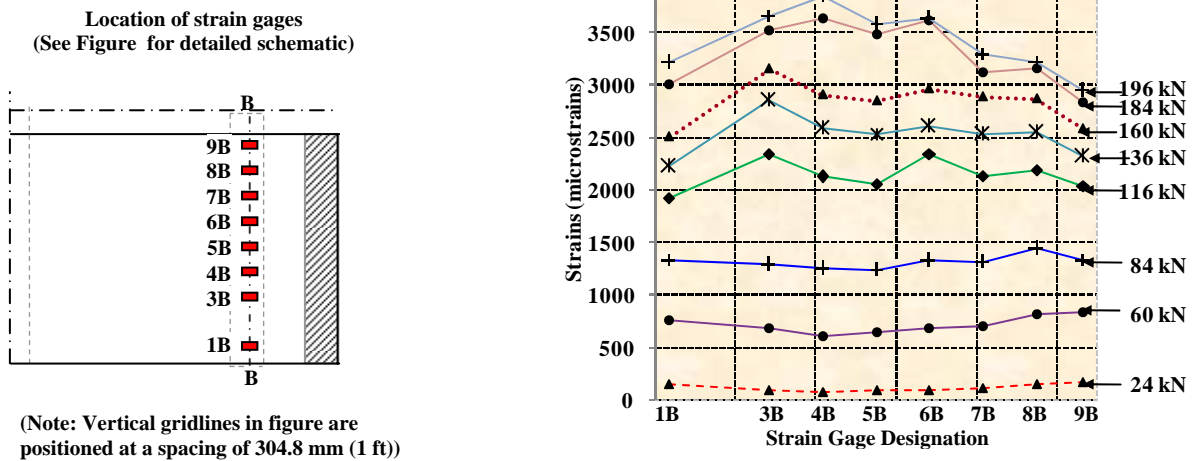


Figure 52: Strains along the edge of the stem wall adjacent to the deck slab overhang (Line B)

Using the strain data throughout the specimen and following a procedure described by Siem et al [24], the shear stress between the concrete and the CFRP strips were calculated using the following equation:

$$\bar{\tau}_{n,n+1} = \frac{(\varepsilon_{n+1} - \varepsilon_n) \cdot E_L \cdot t_L}{(x_{n+1} - x_n)} \quad (11)$$

Where $(x_{n+1} - x_n)$ = distance between two strain gages E_L = the tensile elastic modulus of the CFRP strip and t_L = thickness of the CFRP strips. For these calculations, $E_L = 138.1$ GPa (20.05 Msi) and $t_L = 1.2$ mm (0.047 in) were used for the CFRP strips. The calculated shear stress values within the adhesive are simply the mean value between two strain gages, which ignore localized stress peaks and gradients.

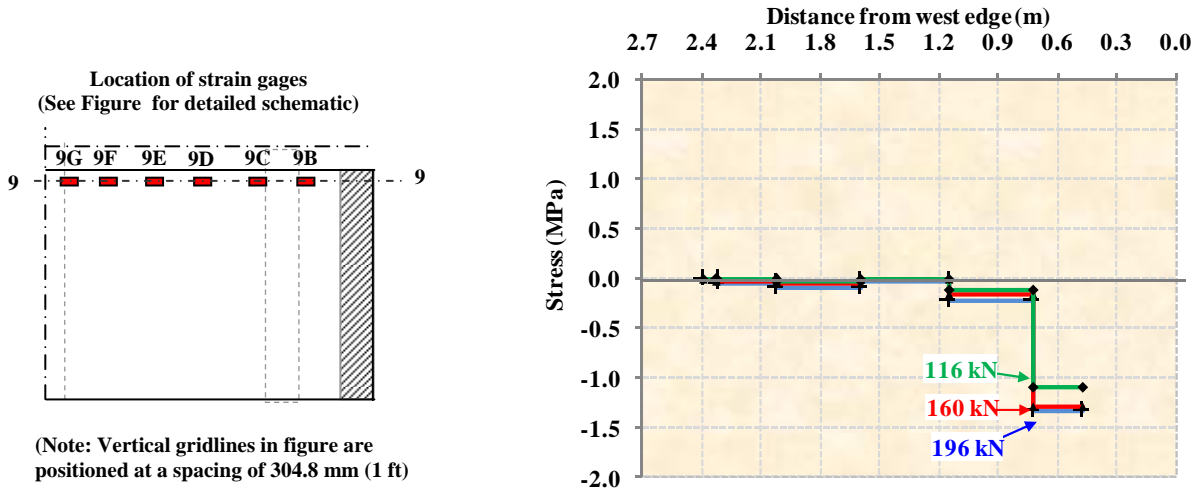


Figure 53: Calculated shear stress within adhesive along the central edge of specimen (Line 9)

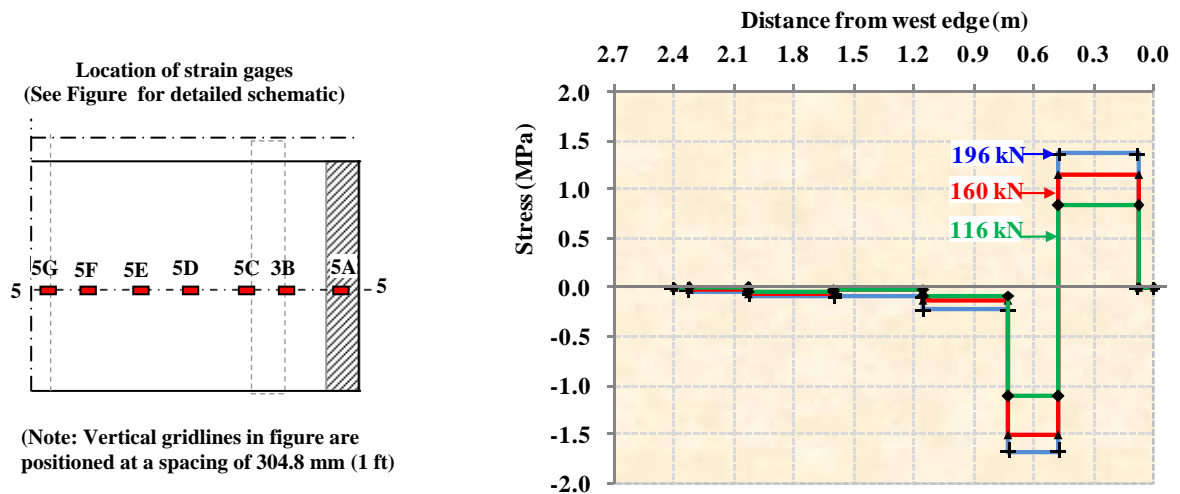


Figure 54: Calculated shear stress within adhesive along the middle of specimen (Line 5)

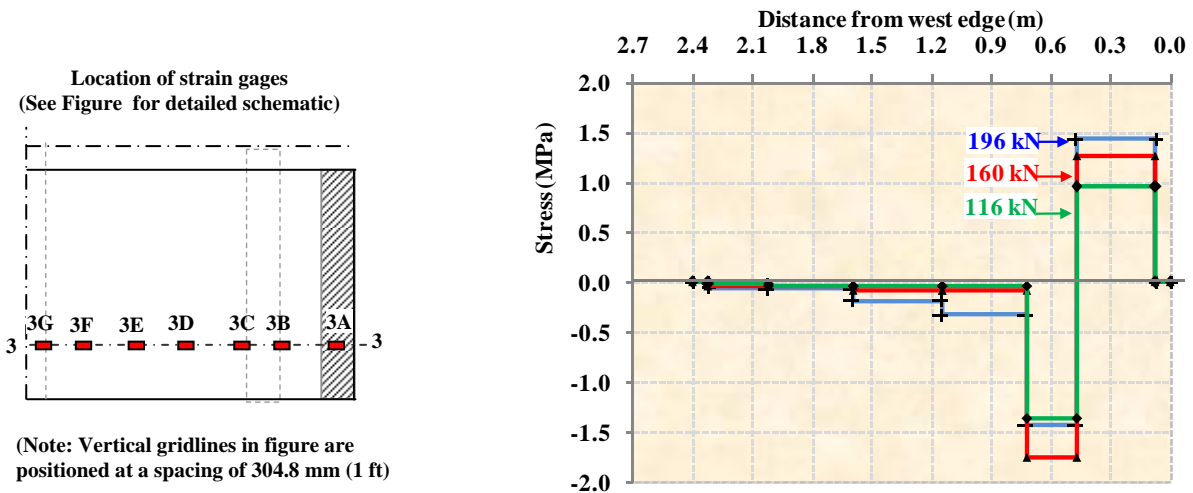


Figure 55: Calculated shear stress within adhesive along an interior CFRP strip (Line 3)

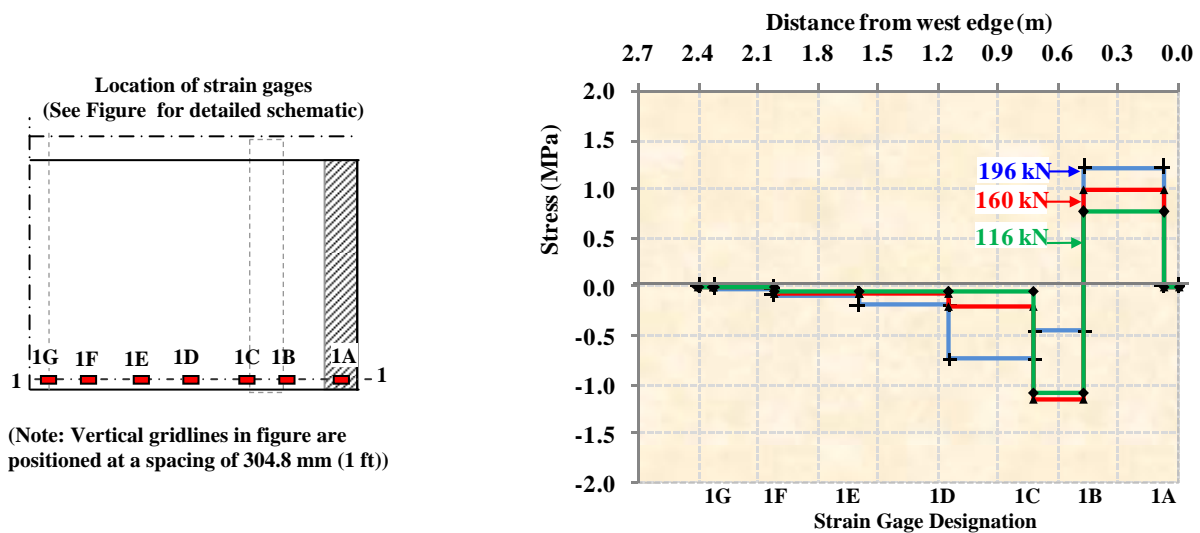


Figure 56: Calculated shear stress within adhesive along the outer edge of specimen (Line 1)

After the testing of the NSM CFRP rehabilitated specimen was completed, the overhang of the specimen was cut off and carefully removed from the rest of the test specimen as shown in Figure 57 to allow for further examination of this critical region.

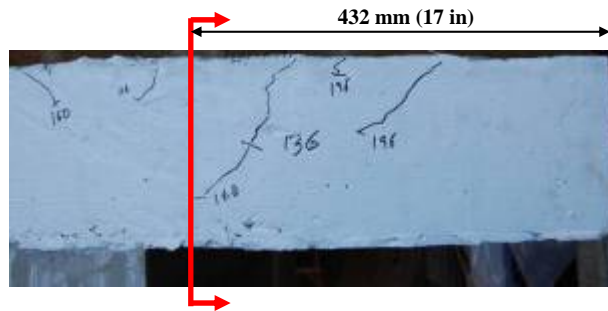


Figure 57: Location of cut for removal of FRP rehabilitated overhang from test specimen

One point of interest to examine on the removed overhang was the actual location of the CFRP strip reinforcement within the section. Figure 58 shows that the actual embedment depth of the near surface mounted CFRP strips was approximately 6 mm (0.25 in) and the actual thickness of the SikaDur 30 resin layer used to bond the CFRP strips to the concrete was also approximately 6 mm (0.25 mm). An embedment depth of 6 mm (0.25 in) is reasonable for NSM applications because it allows enough space for an adequate top surface of resin, which will serve as environmental protection and the wear surface for the deck. However, the 6 mm (0.25 mm) thickness of the SikaDur 30 bottom resin layer exceeded the maximum manufacturer recommended value of 3 mm (1/8 inch). While the current system performed very well the use of an overly thick resin layer could have had a negative effect on the overall structural response of the system.



Figure 58: Detail showing actual location of reinforcement

Figure 59 shows the failure surface of an FRP strip, which has been detached from the top surface of the deck. The center portion of the strip with the firmly attached concrete was the region in which the interfacial failure in the concrete occurred, while the outer sections of the strip were neatly detached from the resin system, due to the method of removal of the strip.



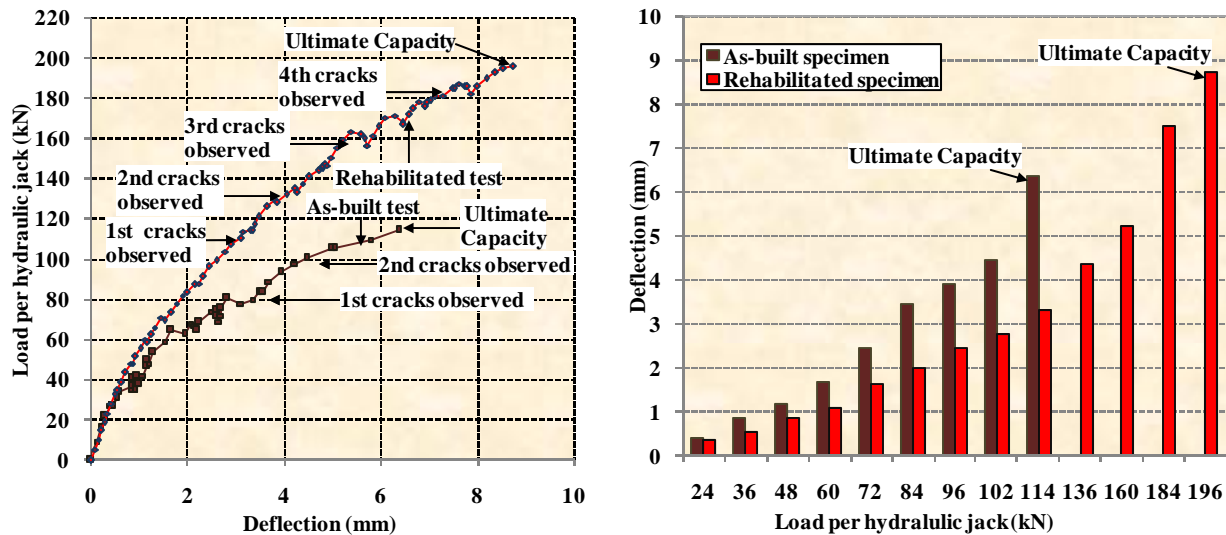
Figure 59: Detail of failure surface of FRP strip

5.8 Comparison with Theory

The NSM CFRP rehabilitated specimen reached ultimate capacity under an applied load of 196 kN (44 kip) per hydraulic jack which is equivalent to an applied moment of 189.2 kN-m (139.2 kip-ft). This improved performance corresponds to a 72 % increase in ultimate capacity over the as-built specimen, which failed under an applied load of 114 kN (26 kip) corresponding to an applied moment of 110.0 kN-m (81.0 kip-ft). The ACI 440-02 calculation for externally bonded FRP reinforcement predicted a maximum moment capacity of 166.0 kN-m (122.4 kip-ft), which corresponds to a 51 % increase in load carrying capacity over the experimentally determined capacity of the as-built specimen. The moment curvature analysis predicted a maximum moment capacity of 185.5 kN-m (136.4 kip-ft), which corresponds to a 69 % increase in load carrying capacity over the as-built specimen. The theoretical predictions and experimental results were within 12 % using the ACI 440 approach and were in close agreement with only a 2 % error using the moment curvature analysis. The larger disagreement with experimental data found from the ACI 440 moment capacity increase equation likely exists because this calculation is a more simplified approach that does not take into account the over strength of the steel reinforcement.

5.9 Comparison with As-Built

The ultimate capacity of the near surface mounted CFRP strip rehabilitated slab was reached at an applied load of 196 kN (44 kips), equivalent to a uniform distributed load of 245 kN/m (16.8 kip/ft), which is 11x the nominal soundwall load. This ultimate capacity is 78% greater than that obtained by the as-built specimen, which occurred at 114 kN (26 kips) per hydraulic jack, equivalent to a uniform distributed load of 142.5 kN/m (9.8 kip/ft), which is 6.33x the nominal wall load. The center deflections under the loading beam for both specimens over the complete loading ranges applied are compared in Figure 60(a) and Figure 60(b). At the failure load level of the as-built specimen, the as-built specimen had a center deflection under the loading beam of 6.36 mm (0.25 in) whereas the FRP rehabilitated specimen deflected approximately half that of the as-built specimen, or 3.33 mm (0.13 in). At ultimate capacity of the FRP rehabilitated specimen, the center deflection under the loading beam was 8.73 mm (0.34 in), which indicates the rehabilitated specimen exhibited a 31.8% increase in deformation capacity over the as-built specimen.



a) Load versus deflection profiles (b) Comparison of linear potentiometers below loading beam

Figure 60: Comparisons of middle center deflections of the deck slab overhang

In addition to increasing the overall load and deformation capacity of the system, the near surface mounted CFRP strips act to increase the stiffness and improve the stability of the system.

The load versus deflection profile shown in Figure 60(a), shows the significantly increased stiffness and more linear profile for the FRP rehabilitated specimen over the as-built specimen.

The deflection profile comparison at the 114 kN (26 kips) per jack load level along the middle of the two slabs is shown in Figure 61. This figure illustrates that for the same load level, the deflections within the FRP rehabilitated specimen are lower than the deflections of the as-built specimen throughout the deck slab and not just at the point of load application.

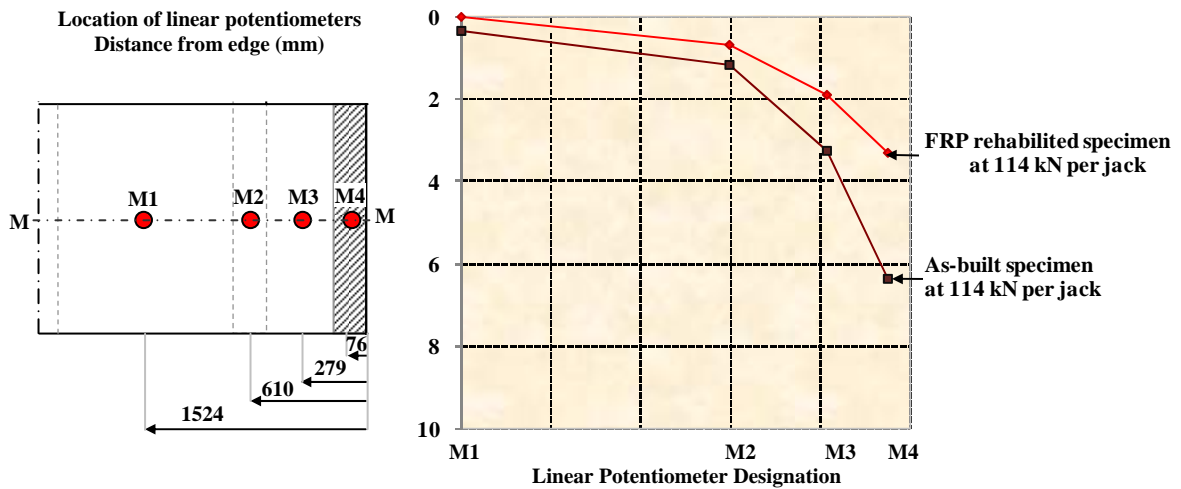


Figure 61: Comparison of deflection profiles along center of specimens (Line M)

The first set cracking observed on the as-built specimen occurred at the load level of 84 kN (19 kip), whereas the first set cracking observed on the FRP rehabilitated specimen occurred at 116 kN (26 kip), which corresponds to a 38% greater load. A comparison of the deflection profiles along the center of the specimens at these loading levels shown in Figure 62 reveals nearly identical deformations for the two specimens.

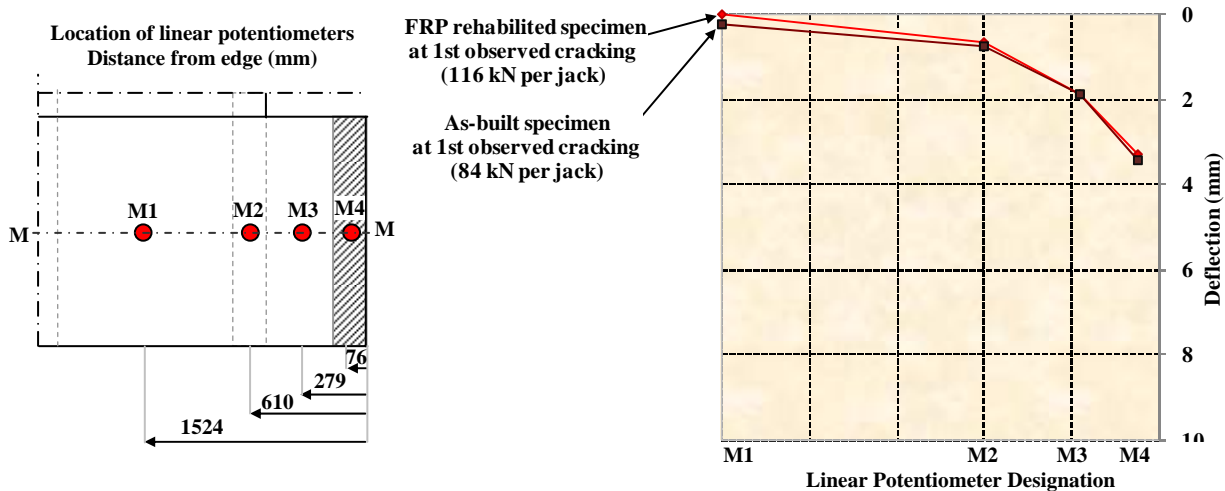


Figure 62: Comparison of center deflection profiles at 1st observed cracking loads (Line M)

The second set of cracking observed on the as-built specimen occurred at the load level of 101 kN (23 kip), whereas the second set of cracking observed on the FRP rehabilitated specimen occurred at 136 kN (31 kip), which corresponds to a 35% greater load. The deflection profile comparison at the load levels where the second set of cracking was observed in Figure 64 also exhibits nearly identical deformations for the two specimens. This indicates that while the FRP reinforcement acts to stiffen the system and increase the load carrying capacity of the overhang region, the shape of the deflection response profile of the system is not modified significantly with the addition of the CFRP strips.

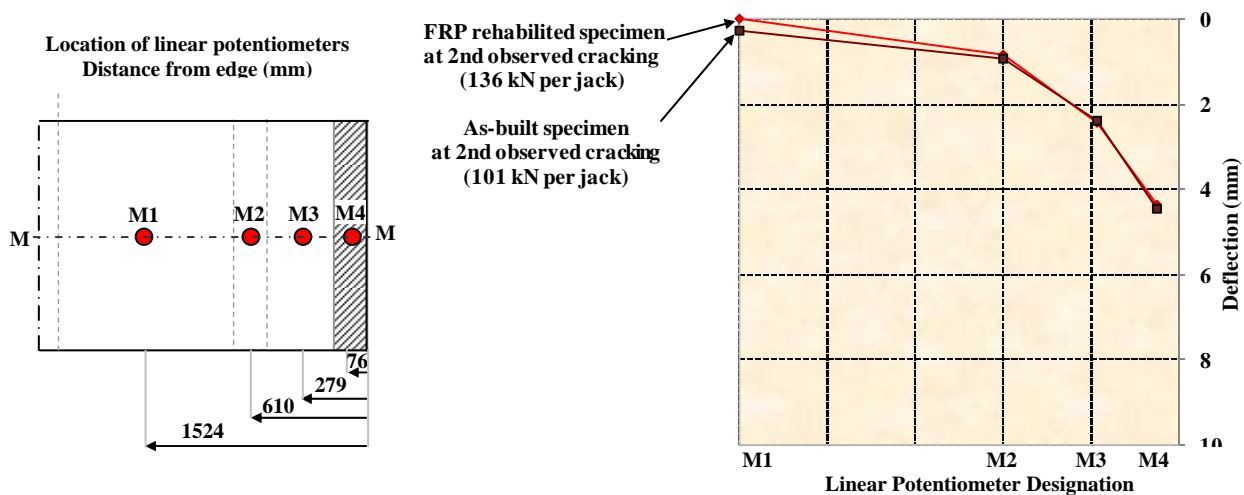


Figure 63: Comparison of center deflection profiles at 2nd observed cracking loads (Line M)

Figure 64 shows the side by side top decks of the two specimens after testing has been completed and all loose concrete on the top deck removed. Details of the critical region of the as-built and FRP rehabilitated top deck are shown in Figure 65 and Figure 66 respectively.



Figure 64: Top view of deck slab tested to ultimate capacity after removal of loose concrete

For the as-built specimen, extensive damage and spalling of the concrete on the top of the deck slab was seen. Yielding in the transverse steel reinforcement followed by loss of aggregate interlock, resulting in failure was observed.



Figure 65: Detail of cracking observed at ultimate capacity- top view of as-built deck

For the FRP rehabilitated specimen, negligible spalled concrete and loose concrete rubble was detected. A concrete splitting failure mode was observed in the FRP rehabilitated specimen.



Figure 66: Detail of cracking observed at ultimate capacity- top view of FRP rehabilitated deck

6. SUMMARY OF RESULTS AND RECOMMENDATIONS FOR FUTURE RESEARCH

Experimental results from the testing of the rehabilitated specimen indicate that the NSMR strengthening scheme was successful at achieving the desired load carrying capacity increase. The ultimate load carrying capacity of the FRP rehabilitated specimen was 196 kN (44 kips) per hydraulic jack, which was 78% higher than the ultimate load of the as-built specimen of 114 kN (26 kips) per hydraulic jack. This value well exceeded the desired load capacity increase of 29.7% above the experimentally determined capacity of the as-built specimen, exhibited a very stable structural response and increased the deformation capacity of the system. The theoretical moment capacity predictions for the as-built specimen were within 11% and 6.5% of the experimentally determined value using ACI 318 and moment curvature analysis respectively. The theoretical moment capacity predictions for the FRP rehabilitated specimen were within 12% of the experimental value using the modified ACI 440-02 approach and were within 2% using moment curvature analysis.

The NSM FRP rehabilitated specimen exhibits a variety of structural performance improvements over the as-built specimen including increased ultimate load carrying capacity, enhanced deformation capacity and more stable overall structural performance. Design options for the near surface mounted CFRP strengthening schemes allow for great flexibility in terms of tailoring the reinforcement parameters for specific applications. With consideration of the minimal disruption to traffic flow and ease of installation, this system is a viable and very attractive rehabilitation option for bridge deck slab overhangs.

The purpose of Phase 1 was to conduct an experimental analysis of the use of NSM for purposes of strengthening and to provide the basis for the planning of Phase 2 as detailed in the initial proposal submitted to Caltrans. Based on the extensive literature review already conducted (although according to the project funding provided by Caltrans is to be completed and reported on in Phase 2) and on the experimental results the following aspects are recommended for further study in Phase 2

- Complete review of the failure modes and mechanisms seen with use of bars/rods as compared to flat strips for purposes of documenting advantages of strips. It is noted that a very brief summary is given in the introductory portion of this report.
- Optimization of groove dimensions and spacing for NSM use through both analytical and experimental study
- Study of adhesive rheology and bond quality as well as durability
- Study of minimum development length and effect of insertion into girder stems
- Study of use for specific strengthening applications
- Development of design guide for Caltrans and development of example comparing NSM use to surface bonding.

It is emphasized that the studies should be conducted on specimens of sufficient size since small scale tests are likely to provide erroneous results due to effects of scale and configuration. It is recommended that these tests only be conducted after a review of advances in Europe and Australia are completed and sufficient analytical work is completed on optimization of groove dimensions and spacing. Since the efficacy of the method is intrinsically related to the ability of the adhesive to not only bond the reinforcement to the concrete substrate but to also enable efficient stress transfer study also needs to be conducted on adhesive rheology, performance characteristics and cure. It is recommended that this be based on the completed durability study which should provide a base-line for further study. Also since it is likely that the NSM will be covered by asphalt the effect of heat due to asphalt on the adhesive and bond should also be studied.

7. REFERENCES

- [1] V.M. Karbhari and L. Zhao, "Use of composites for 21st century civil infrastructure". Computer Method Appl. Mech. Eng. 185 pp. 433–454. (2000)
- [2] S. Rizkalla, T. Hassan, N. Hassan, "Design recommendations for the use of FRP for strengthening of concrete structures" Prog. Struct. Engng Mater. 5 pp. 16–28 (2003)
- [3] K. K. Ghosh, "Assessment of FRP composite strengthened reinforced concrete bridge structures at the component and systems level through progressive damage and non-destructive evaluation (NDE) [Ph.D. dissertation] University of California, San Diego. (2006)
- [4] L. De. Lorenzis, J.G. Teng, "Near-surface mounted FRP reinforcement: An emerging technique for strengthening structures" Composites Part B 38 pp. 119-143 (2007)
- [5] R. Parretti, A. Nanni "Strengthening of RC Members Using Near-Surface Mounted FRP Composites: Design Overview" Advances in Structural Engineering 7, 5 pp. 1-16 (2004)
- [6] J. R. Yost, S. P. Gross, D. W. Dinehart, and J. J. Mildenberg "Flexural Behavior of Concrete Beams Strengthened with Near-Surface-Mounted CFRP Strips" ACI Structural Journal July-August pp. 430-437(2007)
- [7] L. A. DeLorenzis, A. Nanni, and A. L. Tegila, "Flexural and Shear Strengthening of Reinforced Concrete Structures with Near Surface Mounted FRP Bars," Proceedings of the 3rd International Conference on Advanced Composite Materials in Bridges and Structures, Ottawa, Canada, Aug. 15-18, pp. 521-528. (2000)
- [8] El-Hacha, R., and Rizkalla, S., 2004, "Near-Surface-Mounted Fiber- Reinforced Polymer Reinforcements for Flexural Strengthening of Concrete Structures," ACI Structural Journal, V. 101, V. 5, Sept.-Oct., pp. 717-726.
- [9] R. Parretti and A. Nanni "Strengthening of RC Members Using Near-Surface Mounted FRP Composites: Design Overview" Advances in Structural Engineering V. 7 (5) (2004)

- [10] E. Bonaldo, J. A. Oliveira de Barros; and P. B. Lourenço “Efficient Strengthening Technique to Increase the Flexural Resistance of Existing RC Slabs” ASCE Journal of Composites for Construction. March/April pp.149-159 (2008)
- [11] The Concrete Society. Design Guidance for Strengthening Concrete Structures using Fibre Composite Materials. Concrete Society Technical Report 55, 2nd Edition (2004)
- [12] ACI Committee 440. Guide for the Design and Construction of Externally Bonded FRP Systems for Strengthening Concrete Structures. ACI 440.2 R-02. (2002)
- [13] Canadian Standards Association. Canadian Highway Bridge Design Code- Section 16: Fibre-Reinforced Structures (2006)
- [14] AASHTO. LRFD bridge design specifications, 3rd Ed., AASHTO, Washington D.C. (2004)
- [15] A. B. Pridmore, V. M. Karbhari. “Evaluation of Prefabricated FRP Structural Formwork Bridge Deck Systems”. SAMPE 53rd International Technical Conference (2008)
- [16] Caltrans, “Memo to Designers: 22-1. Soundwall Design Criteria” (2004)
- [17] ACI 318-08. Building Code Requirements for Structural Concrete (2008)
- [18] Caltrans Bridge Design Specifications, Section 8- Reinforced Concrete (2003)
- [19] Bentz, E. and Collins M. P. “RESPONSE-2000—Reinforced Concrete Sectional Analysis using the Modified Compression Field Theory” Version 1.0.5. Toronto, Canada. (2000)
- [20] Caltrans, “Memo to Designers: 22-1. Soundwall Design Criteria” (2004)
- [21] Sika Corporation. Product Data Sheet for Sika CarboDur Rods- carbon fiber rods for structural strengthening. Edition 9 (2003)
- [22] Sika Corporation. Product Data Sheet for Sika CarboDur- Carbon fiber laminate for structural strengthening. Edition 7.22 (2005)
- [23] Hughes Brothers, Inc. Product data sheet for Aslan 500- CFRP tape. www.hughesbros.com (2002)

- [24] W. Seim, Y. Vasquez, V.M. Karbhari and F. Seible, "Post-Strengthening of Concrete Slabs: Full Scale Testing and Design Recommendation," ASCE Journal of Structural Engineering, 129[6], pp. 743-752 (2003)
- [25] W. Seim, M. Hormann, V.M. Karbhari and F. Seible, "External FRP Poststrengthening of Scaled Concrete Slabs" ASCE Journal of Composites in Construction, 5[2] pp. 67-75 (2001)
- [26] Sika Europe- German Institute of Construction Technology, 1998
- [27] International Concrete Repair Institute, ICRI Guideline No. 037324, "Selecting and Specifying Concrete Surface Preparation for Sealers, Coatings, and Polymer Overlays" (1997)
- [28] S. J. Jin. "Statistical Characterization of Prefabricated FRP Composite Materials for Rehabilitation of Concrete Structures". Master Thesis; Department of Structural Engineering, University of California, San Diego. (2008)
- [29] Sika Corporation "CarboDur Installation Guide" Sika construction documents